HOKKAIDO UNIVERSITY

Title	Structural Analyses of Helices of Poly-Oligo(lactic acid) in Solution-State
Author(s)	本元, 貴大
Degree Grantor	北海道大学
Degree Name	博士(生命科学)
Dissertation Number	甲第13161号
Issue Date	2018-03-22
DOI	https://doi.org/10.14943/doctoral.k13161
Doc URL	https://hdl.handle.net/2115/69967
Type	doctoral thesis
File Information	Takahiro_Hongen.pdf

Hokkaido University Collection of Scholarly and Academic Papers : HUSCAP

Doctoral Thesis, 2018

Structural Analyses of Helices of Poly- Oligo(lactic acid) in Solution-State

(液相中ポリ・オリゴ乳酸のらせん構造解析)

Takahiro Hongen

Hokkaido University Graduate School of Life Science

2018 March

平成 29 年度博士論文

液相中ポリ・オリゴ乳酸のらせん構造解析

本元　貴大

北海道大学大学院生命科学院

2018 年　3 月

Dedication

This dissertation is dedicated to my family; father Hisao Hongen, mother Ayako Hongen, and younger sister Yo-ko Hongen. Without their supports and encouragements, the study described would not have been successful.

Acknowledgements

First of all, I wish to express my profound gratitude to chief examiner Prof. Kenji Monde (Hokkaido University) for guidance over six years, in which he has given valuable opportunities to go various conferences and to acquire a broad range of knowledge and advanced expertise. In addition, I would like to express my sincere gratitude to Prof. Tohru Taniguchi (Hokkaido University) and Prof. Yuta Murai (Hokkaido University) for experimental guidance and encouragements. I am also thankful to Prof. Shin-Ichiro Nishimura (Hokkaido University) and Hiroshi Hinou (Hokkaido University) for helpful discussions. I have benefited from Academic Researcher Kazuhiko Orito (Hokkaido University) for suggestive experimental advices. In addition, I am grateful to Prof. Makoto Demura (Hokkaido University) for examinations of this thesis.

I wish to thank Prof. Jun-Ichi Kadokawa (Kagoshima University) and Dr. Shintaro Nomura (Kagoshima University) for synthesizing PLLA-Amylose complex and helpful discussions on conformational analysis on PLLA.

I am grateful to Monde Laboratory members, Dr. Mostafa A. S. hammam (Currently, King Faisal University, Saudi Arabia), Dr. Ananda Kumer C. S., Dr. Attila Mandi, Dr. Shota Saito (Currently, TechnoPro R & D, Inc.), Mr. Enkhsukh Lkhamkhuu, Dr. Siddabasave Gowda B, Mr. Deepak H. V., Mr. Mahadeva Swamy M. M., Mr. Koolath Sajeer, Ms. Aimi Suhaily Saadin, Mr. Aqmal Othman, Ms. Enkhmaa Enkhbat, Ms. Kie Nakano, Ms. Mai Asahata, Ms. Haruka Satoh, Mr. Tomofumi Sakai. Mr. Shota Hashino, Ms. Mari Takimoto, Mr. Ryosuke Baba, Ms. Taeko Hirakawa, Mr. Takuya Ishikawa, Mr. Ren Ogawa, Mr. Takuya Kitahara, Mr. Yuma Kobayashi, Ms. Aya Hashimoto, Mr.

Takahiro Suzuki, Mr. Tomoya Suzuki, Mr. Shohei Fujita, Ms. Haruka Murabayashi, Mr. Akihiro Sekiguchi, Mr. Takahiro Kitahara, Mr. Yoshihiro Abe, and Mr. Yuki Watanabe. My special thanks are due to secretaries, Ms. Asana Sugawara, and Ms. Yoshiko Suga, and Ms. Keiko Abe.

I wish specially thank to my collegues, Mr. Shingo Takiguchi (Currently, DAIICHISANKYO RD NOVARE CO., LTD), Mr. Keishiro Shibata, and Ms. Keiko Yamane for their discussions, enciuragements, and spiritual supports.

Finally, I gratefully acknowledge a SUNBOR SCHOLARSHIP from SUNTORY FUNDATION FOR LIFE SCIENCE.

Abbreviations

Ac_2O	acetic anhydride
AcOH	acetic acid
AcCl	acetyl chloride
Ag_2O[I]	silver oxide[I]
Ala	alanine
aq	aqueous solution
br	broad
c	concentration
CD	circular dichroism
$CHCl_3$	chloroform
CH_2Cl_2	Dichloromethane
d	doublet
DFT	density functional theory
DHP	3,4-dihydro-2H-pyran
DIPEA	diisopropylethylamine
DMAP	*N*,*N*-dimethyl-4-aminopyridine
DMF	*N*,*N*-dimethylformamide
DMSO	dimethyl sulfoxide
ECD	electronic circular dichroism
ESI	electrospray ionization
Et_3N	triethylamine
EtOAc	ethyl acetate

h hour(s)

HATU 1-[Bis(dimethylamino)methylene]-1H-1,2,3-triazolo[4,5-b]pyridinium 3-oxid hexafluorophosphate

HOBt 1-hydroxybenzotriazole

Hz hertz

IR infrared

l pathlength

Lac lactic unit

m multiplet

MeCN acetonitrile

MeI methyl iodide

MeOH methanol

$MgSO_4$ magnesium sulfate

$NaHCO_3$ sodium hydrogen carbonate

Pd-C 10% paradium on charcoal

$Pd(OH)_2$ Pearlmans' catalyst

PLLA poly-L-lactic acid

PPII polyproline type II

p-TsOH *p*-toluenesulfonic acid

q quartet

THF tetrahydrofuran

THP 2-tetrahydropyranyl group

VCD vibrational circular dichroism

$[\alpha]_D$ specific optical rotation

Chapter 1

General Introduction

1-1 Helices in biomolecules

Helical structure is a common skeleton in biomolecules such as nucleic acids, proteins, sugars and so on. These biomolecules may form multiple helical patterns; for instance, α-helix structure and polyproline type II (PPII) structure are formed as a typical helical structure in the secondary structure of proteins.[1] Under the influence of salt concentration and base sequence, DNA changes to three kinds of helical structures such as A-DNA, B-DNA, and Z-DNA.[2] β-glucan, which is one of sugar chains, it forms a triple helical structure in water, while under DMSO solvent, the triple helix structure is dissolved and changed random coil conformation by intra- or interhydrogen bond (Fig 1.).[3] Understanding the helical structure of each biopolymer is very important to correctly reveal the biological phenomena and analysis of the helical structure is expected to realize new polymer creation that s biological functions.

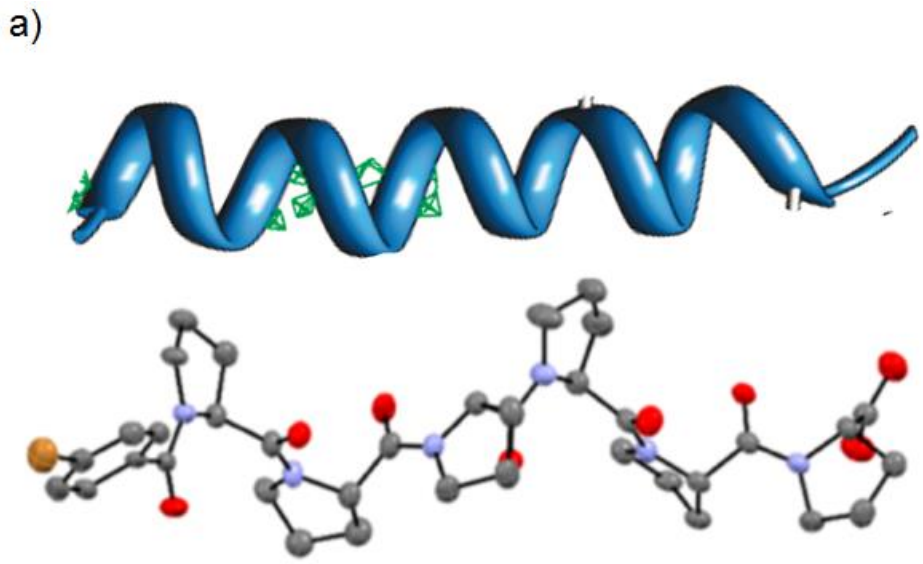

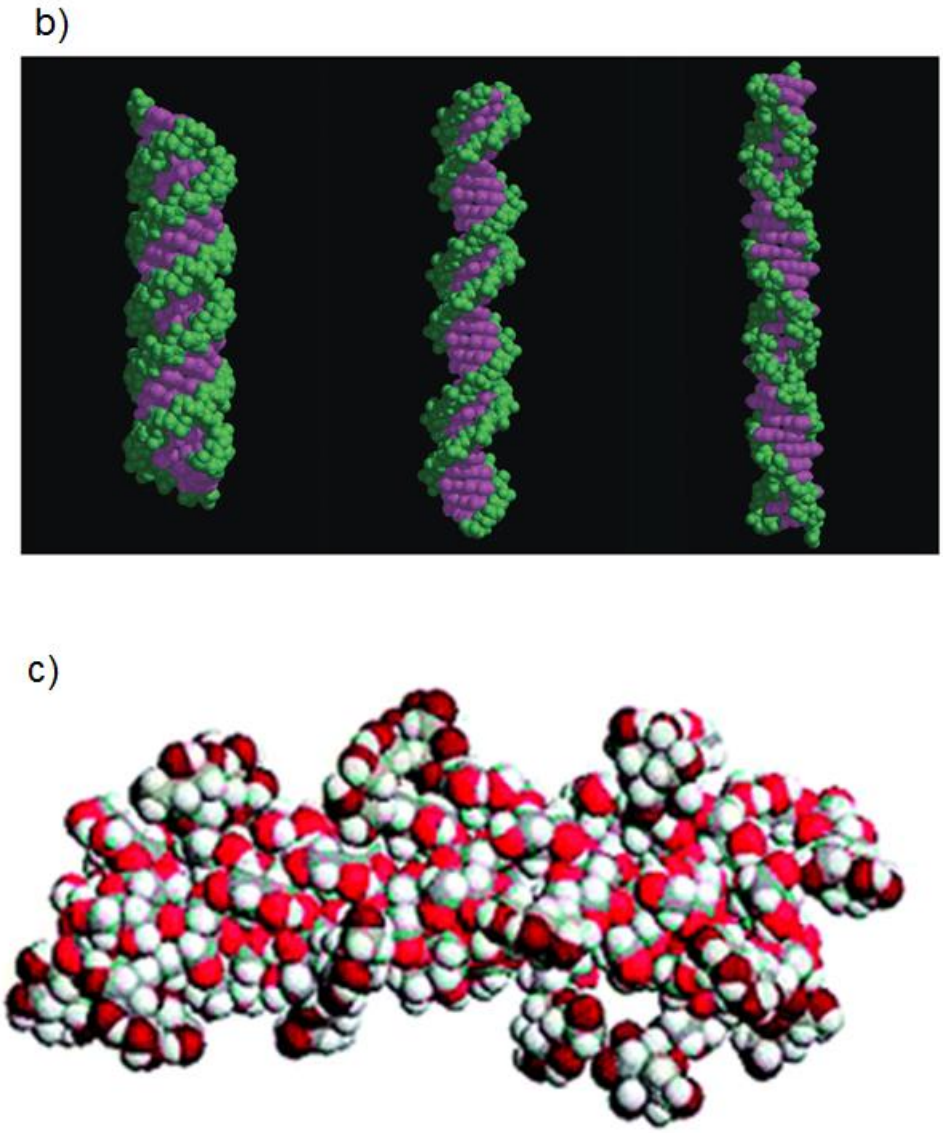

Figure 1. (a) Secondary structure of α-helix (top) and PPII helix (bottom), (b) Structure of A-DNA (left), B-DNA (center), and Z-DNA (right), (c) triple helical structure of β-glucan (schizophyllan)

1-2 Poly Lactic Acid

Poly lactic acid (PLA) is one of the artificial helical macromolecules that have already been used in biochemical and pharmaceutical fields due to their controllable bioaccumulation. PLA is a biocompatible and environmentally benign thermoplastic employed as surgical suture, as implant materials, and in drug delivery systems, exists as a helix in its α-, β-, and γ-crystalline states, and it forms 3_1 or 3_2 helical structure.[4,5] This structure is a common skeleton as PPII structure of proteins and peptides, so PLA is a biodegradable polyester analogue of polypeptide. The similarity of PLA and polyalanine has been suggested over 40 years and the studies on its conformation has been of interest.[4,6] However, the application of PLA to peptidomimetics has been obstructed in part by the lack of a convenient and accurate method to study the solution-state conformation of polyester. The establishment of such a method should not only be useful in clarifying the stereostructure of polyester, but also facilitate biochemical studies of peptides and proteins containing α-hydroxy acid that are present in nature[7] or are produced by genetic code expansion[8,9] or by chemical synthesis.[10,11]

1-3 Spectroscopies for Biomolecules in vibrational circular dichroism (VCD)

Molecular chirality is a fundamental property that governs numerous biological phenomena and is the source of the secondary and higherorder structures of biomolecules. Understanding the chiral structures of nucleic acids, proteins, saccharides and lipids should provide detailed insights into biological systems and help create artificial molecules that mimic or exceed the functions of biomolecules. However, despite extensive studies on chirality, our current level of knowledge does not allow us to thoroughly understand and mimic biomolecular structures, which is partially due to the lack of convenient techniques for analyzing molecular stereostructures. X-ray diffraction analysis has been used to obtain detailed structural data of various molecules, but its efficacy has been limited due to the requirement of a fine crystal. Moreover, this method does not provide structural information in solution. On the other hand, the applicability of solution-state nuclear magnetic resonance spectroscopy is primarily limited to molecules in which hydrogen atoms are suitably located. To understand the details of biological systems, our laboratory have been applying vibrational circular dichroism (VCD) spectroscopy[12–14] to analyze the three-dimensional structures of various biomolecules. For virtually all chiral organic molecules, VCD spectroscopy is capable of detecting signals whose shape reflects their stereostructure.

Circular dichroism spectroscopy, which is a measurement of the difference in the absorptions of a chiral sample toward left versus right circularly polarized light, is sensitive to molecular configuration and conformation including subtle structural changes in polymers. Conventional circular dichroism using ultraviolet–visible light, occasionally referred to as electronic circular dichroism (ECD) (Figure 2), has been applied to the conformational analysis of various polymers, such as proteins, nucleic

acids, artificial polymers and supramolecules.[15] However, the applicability of ECD spectroscopy is limited to molecules that contain UV chromophores. VCD is a type of circular dichroism spectroscopy based on infrared radiation and has several advantages over conventional ECD. First, the use of infrared radiation allows for the application of VCD spectroscopy to virtually all chiral organic molecules. Second, VCD can acquire numerous signals that reflect the molecular stereostructure over a wide frequency region. Finally, VCD exhibits superior accuracy for spectral prediction by using theoretical calculations, which leads to the elucidation of detailed molecular structures.

As an example of the determination of the configuration of a small molecule, Figure 3 shows a comparison of the experimentally observed spectra and the theoretically predicted ones using the density functional theory (DFT) calculations of α-pinene (1). The observed VCD spectrum of (+)-1 exhibited good agreement with the calculated one for (1R,5R)-1 in terms of the peak positions, relative intensities and signs of each signal. Meanwhile, the experimental VCD spectrum for (−)-1 exhibited a pattern that was the mirror image of the theoretical spectrum. These comparisons enable one to elucidate the structures of (+)-1 as 1R,5R and (−)-1 as 1S,5S.

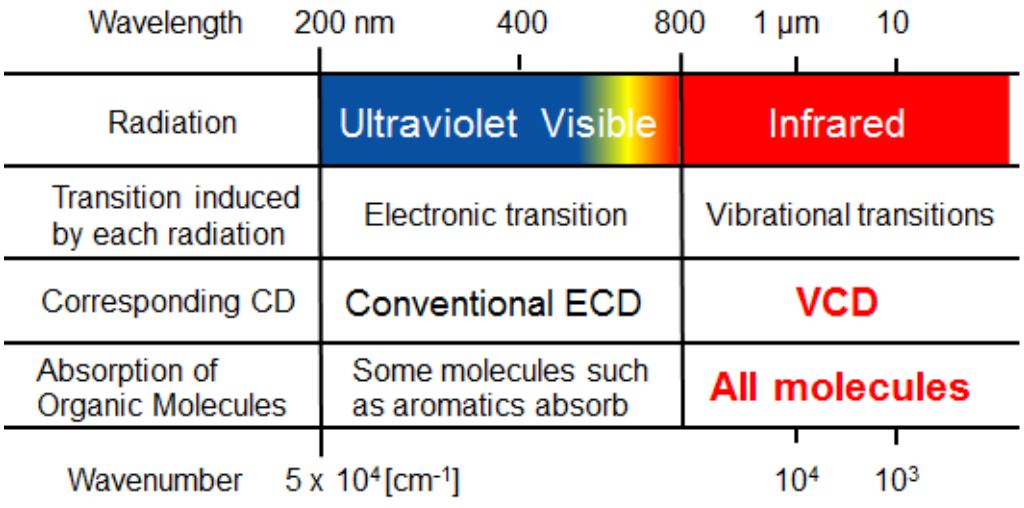

Figure 2. Comparison of CD and VCD

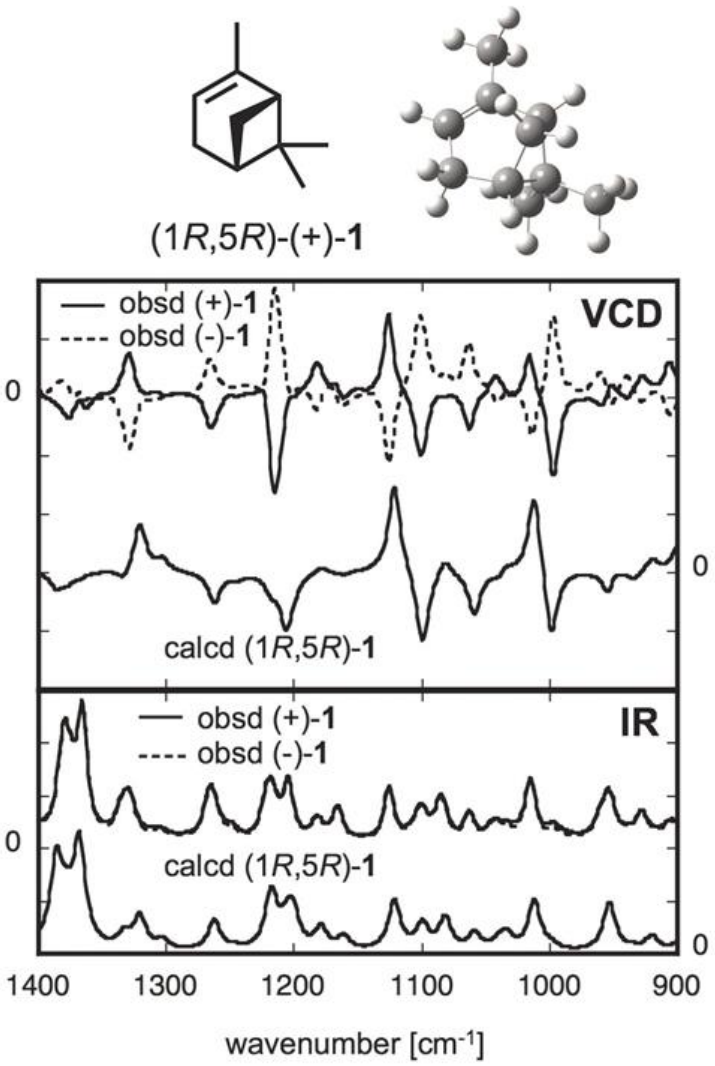

Figure 3. Comparison of the observed and calculated VCD (top) and IR (bottom) spectra of α-pinene

VCD exciton chirality method

Even without theoretical calculations, VCD spectroscopy has been employed to study the structure of various biomacromolecules in an empirical manner.[16] In particular, since the early days of VCD spectroscopy, it has been proposed that a pair of carbonyl groups may give rise to a characteristic VCD signal whose shape is indicative of the spatial relationship of the C=O groups.[17,18] Recently, we examined this phenomenon in detail

and established a method, which is tentatively referred to as a VCD exciton chirality method (named after the ECD exciton chirality method)[19,20] to determine the molecular structure without theoretical calculations.[21] When the absolute twist of the two carbonyl groups is positive ($0°<\theta<+180°$), a positive–negative (from lower to higher frequency) VCD couplet is observed; meanwhile, a negative twist ($-180°<\theta<0°$) yields a negative–positive couplet (Figure 4a). This couplet is due to a through-bond and/or through-space interaction between the two C=O chromophores. As shown in Figure 4b, monocarbonyl sugar derivatives 4a and 4b exhibited almost flat VCD features in the C=O stretching region (1600–1800 cm^{-1}). However, biscarbonyl 4c exhibited an intense VCD couplet whose sign is consistent with the counterclockwise orientation of the two C=O groups. The interaction between carbonyl groups becomes weaker as the distance between the two carbonyl groups increases, and therefore, the contribution of two distant carbonyl groups to an observed couplet is often negligible.[21,22] Accordingly, even if the main chain of a polymer contains numerous carbonyl groups, its observed VCD couplet would be primarily governed by the interactions between pairs of adjacent carbonyl groups. Although the current application of this approach has been limited to a molecule with C=O or other functional groups, this method is applicable to large molecules that are beyond the scope of theoretical calculations.

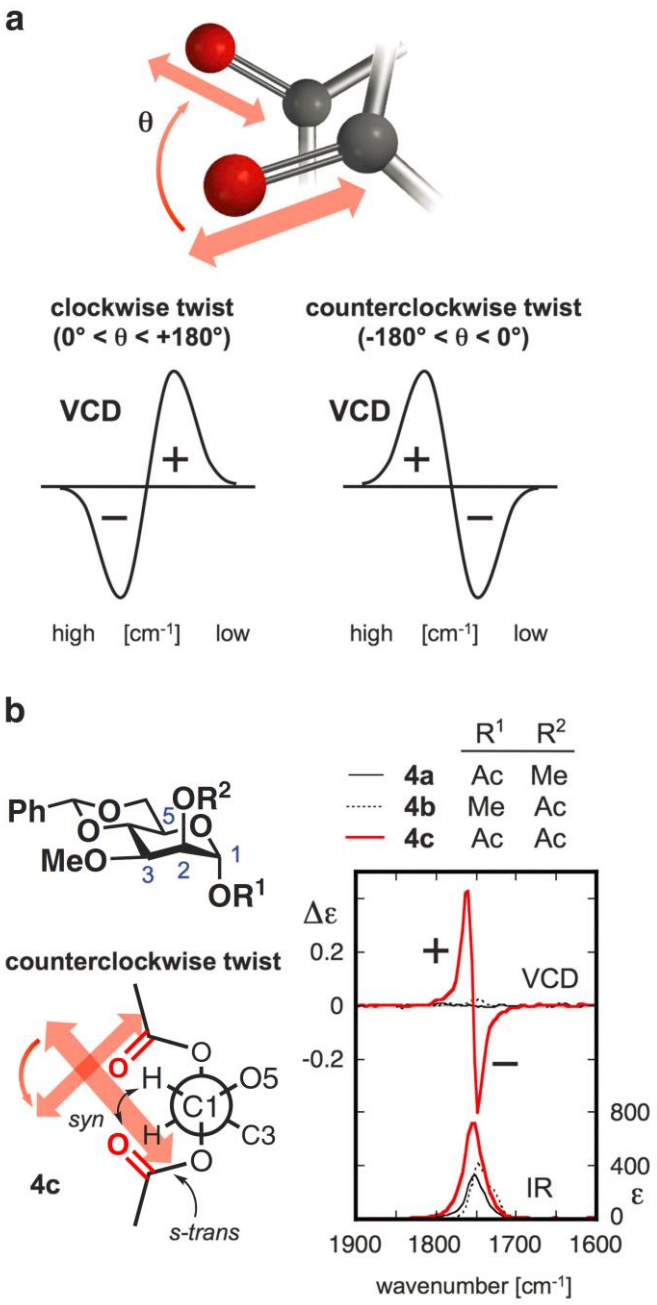

Figure 4. (a) Interaction of two carbonyl groups and the resulting VCD couplet. The sign of the couplet is governed by the torsion angle (θ) defined by two electric transition moments (red arrows) that are virtually parallel to each C=O bond. (b) Comparison of the VCD spectra of mono- and biscarbonyl sugar derivatives (4a–4c).

Structural analysis of peptide and protein using VCD

VCD spectroscopy has long been used as a powerful tool to study their structures.[16,23] Virtually irrespective of their amino acid sequence, VCD exhibits amide I and II signals characteristic of their secondary structures. The signals in the amide I region are due to C=O stretching vibrations in the amide linkage and the signals in the amide II region originate from N-H deformation and other vibrations. Figure 6a shows a typical example of the VCD spectral features of representative polypeptides measured in H_2O. It is important to note that the spectral shapes are different in D_2O, especially in the amide II region.[16] In H_2O, the right-handed α-helix and 3_{10} helix typically exhibit a positive–negative couplet in the amide I region and a negative band in the amide II region. In contrast, the left-handed PPII helix exhibits a negative–positive couplet in the amide I region, which is characteristic of the counterclockwise orientation of a pair of adjacent carbonyl groups. Interestingly, the VCD features of random coil closely resemble those of the PPII helix. On the basis of this observation, a random coil has been proposed to contain a large fraction of local lefthanded helices.[24] A β-sheet structure may yield a negative band in the amide I region, which in some cases is associated with negative and positive signals in the amide II region. Further structural details regarding a specific type of ß-sheet (for example, parallel and antiparallel, in-register and out-of-register, and intersheet stacking patterns) may be obtained using theoretical simulations and/or isotope labeling.[25,26] When a polypeptide forms a fibril structure, it yields hugebisignate C=O stretching VCD signals whose shapes are completely different from the representative patterns for any known secondary structures.[27]

Figure 5b shows the IR and VCD spectra of a glycopeptide with antifreeze activity (5a) measured in H_2O. The disaccharide attached to threonine is essential for the formation

of its left-handed polyproline type II helix secondary structure as well as its antifreeze activity.[28] The VCD spectrum of 5a contains a negative–positive C=O VCD couplet (1639 and 1670 cm^{-1}), which is indicative of its PPII helical structure. A negative VCD band observed at 1165 cm^{-1} was assigned as vibrational motions that are characteristic of the α-glycosidic linkage of N-acetylgalactosamine.[29] The VCD spectrum of tripeptide unit 5b did not show any strong signals in the C=O stretching region, which is consistent with its unordered structure.[28]

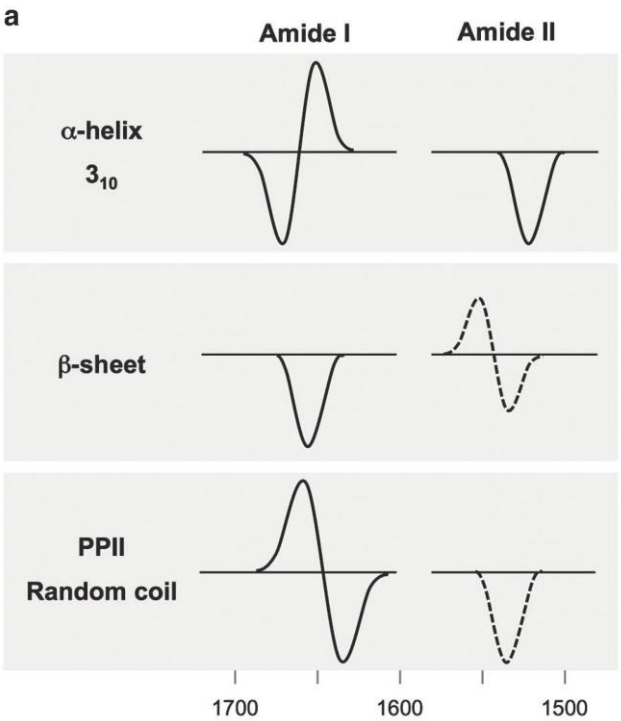

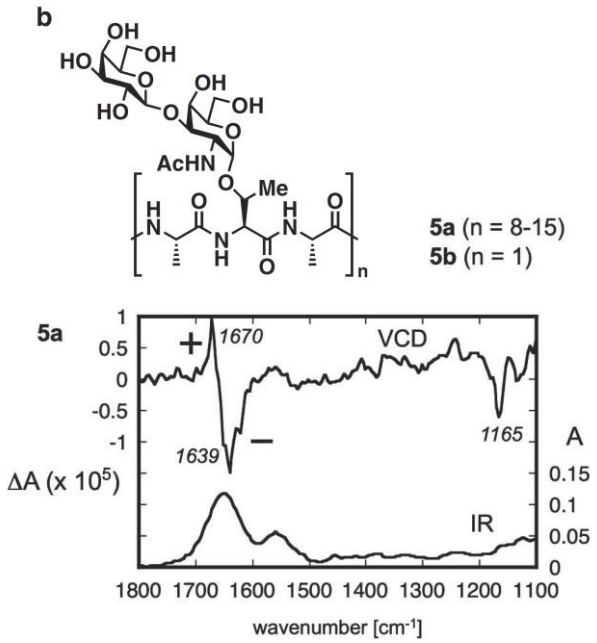

Figure 6. (a) Representative VCD patterns of polypeptides in the amide I and II regions in H_2O. (b) VCD and IR spectra of glycopeptide antifreeze glycoprotein (AFGP) oligomer (6a)

1-4 Structural analyses of helical structure toward polymer and its derivative using VCD

It has not been clarified whether the three-dimensional structure of poly-L-lactic acid in the liquid phase forms a left handed 31 helical structure as in the solid phase state. Therefore, if it is found that the poly (L-lactic acid) forms the structure, it can be combined with a peptide forming a PPII structure which is also a left-handed 31 helical structure to newly respond to the human living things It is expected to lead to the creation of polymers. Therefore, this thesis was aimed at the detailed three-dimensional structure analysis of poly-L-lactic acid in the liquid phase and the application to the secondary structure analysis of poly-L-lactic acid-polypeptide derivatives.

In Chapter 2, I describe the conformational analysis of poly lactic acid by VCD. To demonstrate the utility of VCD technique for conformational study of polyester, we hereby present a VCD study of the structural analysis of poly(L-lactide) (PLLA), PLLA-amylose complex, and oligo(Llactic acid)s (structures and notations are shown in Figure 1) using both the analysis of VCD exciton couplet and density functional theory (DFT) calculation. Another objective of this work is to address the conformational details of PLA in an isolated state and in a complex with other molecules, which should advance the peptidomimetic application of lactic acid.

In Chapter 3, I describe controlling oligoalanine conformation by replacement of amide to ester linkeage. Oligo(lactic acid) is an ester-analogue of short oligoalanine sequence and adopts a rigid left-handed helical structure. In this study, oligo(lactic acid) was incorporated into oligoalanine sequences and their conformations were studied by vibrational circular dichroism and electronic circular dichroism spectroscopy. The results suggested that oligo(lactic acid) moiety in these sequences maintain a left-handed helix

and increase the conformational propensity of the oligoalanine moiety to form a left-handed PPII-like helix. The importance of the chirality of oligo(lactic acid) moiety for the oligoalanine conformation was also studied. The results obtained in this study should be useful in developing ester-containing oligopeptides that function better than normal peptides.

1-5 references

1 (a) Xiong, K.; Asciutto, E. K.; Madura, J. D.; Asher, S. A. *Biochemistry* **2009**, *48*, 10818–10826. (b) Wilhelm, P.; Lewandowski, B.; Trapp, N.; Wennemers, H. *J. Am. Chem. Soc.* **2014**, *136*, 15829−15832.

2 https://www.mun.ca/biology/scarr/iGen3_02-14.html

3 (a) Xu, X.; Zhang, X.; Zhang, L.; Wu, C. *Biomacromolecules* **2004,** *5*, 1893-1898. (b) Okobira, T.; Miyoshi, K.; Uezu, K.; Sakurai, K.; Shinkai, S. *Biomacromolecules* **2008**, *9*, 783-788.

4 Jiang, X.; Luo, Y.; Tian, X.; Huang, D.; Reddy, N.; Yang, Y. *Chemical Structure of Poly(lactic acid). In Poly(lactic acid): Synthesis, Structures, Properties, Processing, and Applications; Auras*, John Wiley & Sons, **2010**, p 69.

5 Irsai, I.; Majdik, C.; Lupan, A.; Silaghi-Dumitrescu, R. *J. Math. Chem.* **2012**, *50*, 703−733.

6 Brant, D. A.; Tonelli, A. E.; Flory, P. J. *Macromolecules* **1969**, *2*, 228−235.

7 Hubbard, B. K.; Walsh, C. T. *Angew. Chem., Int. Ed.* **2003**, *42*, 730−765.

8 Kobayashi, T.; Yanagisawa, T.; Sakamoto, K.; Yokoyama, S. *J. Mol. Biol.* **2009**, *385*, 1352−1360.

9 Li, Y.-M.; Yang, M.-Y.; Huang, Y.-C.; Li, Y.-T.; Chen, P. R.; Liu, L. *ACS Chem. Biol.* **2012**, *7*, 1015−1022.

10 Deechongkit, S.; Nguyen, H.; Powers, E. T.; Dawson, P. E.; Gruebele, M.; Kelly, J. W. *Nature* **2004**, *430*, 101−105.

11 Eildal, J. N. N.; Hultqvist, G.; Balle, T.; Stuhr-Hansen, N.; Padrah, S.; Gianni, S.; Strømgaard, K.; Jemth, P. *J. Am. Chem. Soc.* **2013**, *135*, 12998−13007.

12 Nafie, L. A. *in Vibrational Optical Activity: Principles and Applications*, Wiley,

Chichester, **2011**.

13 Stephens, P. J., Devlin, F. J. & Cheeseman, J. R. *in VCD Spectroscopy for Organic Chemists*, CRC Press, Boca Raton, FL , **2012**.

14 He, Y., Wang, B., Dukor, R. K. & Nafie, L. A. *Appl. Spectrosc.* **2011**, *65*, 699–723.

15 Taniguchi, T., Usuki, T. *in Supramolecular Chemistry: from Molecules to Nanomaterials*, John Wiley & Sons, **2012**, 2, 393-410.

16 Keiderling, T. A., Lakhani, A. *in Comprehensive Chiroptical Spectroscopy*, Wiley, **2012**, *2*, 707-758.

17 Holzwarth, G. & Chabay, I. *J. Chem. Phys*. **1972**, *57*, 1632–1635.

18 Freedman, T. B. & Nafie, L. A. *Top. Stereochem*. **1987**, *17*, 113–206.

19 Harada, N. & Nakanishi, K. *University Science Books* , **1983**.

20 Harada, N., Nakanishi, K., Berova, N. *in Comprehensive Chiroptical Spectroscopy*, Wiley, **2012**, 2, 115-166.

21 Taniguchi, T. & Monde, K. *J. Am. Chem. Soc.* **2012**, *134*, 3695–3698.

22 Asai, T., Taniguchi, T., Yamamoto, T., Monde, K. & Oshima, Y. *Org. Lett*. **2013**, *15*, 4320–4323.

23 Keiderling, T. A. *Nature* **1986**, *322*, 851–852.

24 Dukor, R. K. & Keiderling, T. A. *Biopolymers* **1991**, *31*, 1747–1761.

25 Welch, W. R. W., Kubelka, J. & Keiderling, T. A. *J. Phys. Chem. B* **2013**, *117*, 10343–10358.

26 Welch, W. R. W., Keiderling, T. A. & Kubelka, J. *J. Phys. Chem. B* **2013**, *117*, 10359–10369.

27 Ma, S., Cao, X., Mak, M., Sadik, A., Walkner, C., Freedman, T. B., Lednev, I. K., Dukor, R. K. & Nafie, L. A. *J. Am. Chem. Soc.* **2007**, *129*, 12364–12365.

28Tachibana, Y., Fletcher, G. L., Fujitani, N., Tsuda, S., Monde, K. & Nishimura, S.-I. *Angew. Chem. Int. Ed. Engl.* **2004**, *43*, 856–862.

29 Monde, K., Taniguchi, T., Miura, N. & Nishimura, S.-I. *J. Am. Chem. Soc*. **2004**, *126*, 9496–9497.

Chapter 2

Detailed Structural Analysis of Poly Lactic Acid by Vibrational Circular Dichroism

2-1 Introduction

As described in Chapter 1, conformational analysis of poly L-lactic acid in the liquid phase has not been reported. The reason for this is that there are different problems with CD or VCD when poly lactic acid is measured. First, when measuring with CD, the absorption intensity of the ester group of the functional group is very small. The ECD signal of ester functional group, whose n → π* transition generally shows very weak absorption at around 210 nm, is not informative for conformational analysis of polyester.[1] In the case of measurement with VCD, since the size of the polymer is very large, it is a problem that the theoretical calculation cannot be performed. Stereostructure analysis of molecules by VCD cannot calculate because the absolute stereochemistry is determined by comparing measured spectra and computed spectra and the number of possible conformations of molecules is too large for large molecular weight polymers. Therefore, in this study, we aimed at establishing a tertiary structure analysis method of secondary structure of polyester of VCD using poly lactic acid as a model compound. First, the VCD spectrum of polylactic acid is measured. Subsequently, oligomers of lactic acid in which the chain length of lactic acid was gradually extended were synthesized, the VCD spectrum was similarly measured, and the correlation with poly lactic acid was verified. Theoretical calculations were carried out on oligomers having a shape similar to the VCD spectrum of poly lactic acid and verified the difference between the measured spectrum and the calculated spectrum.

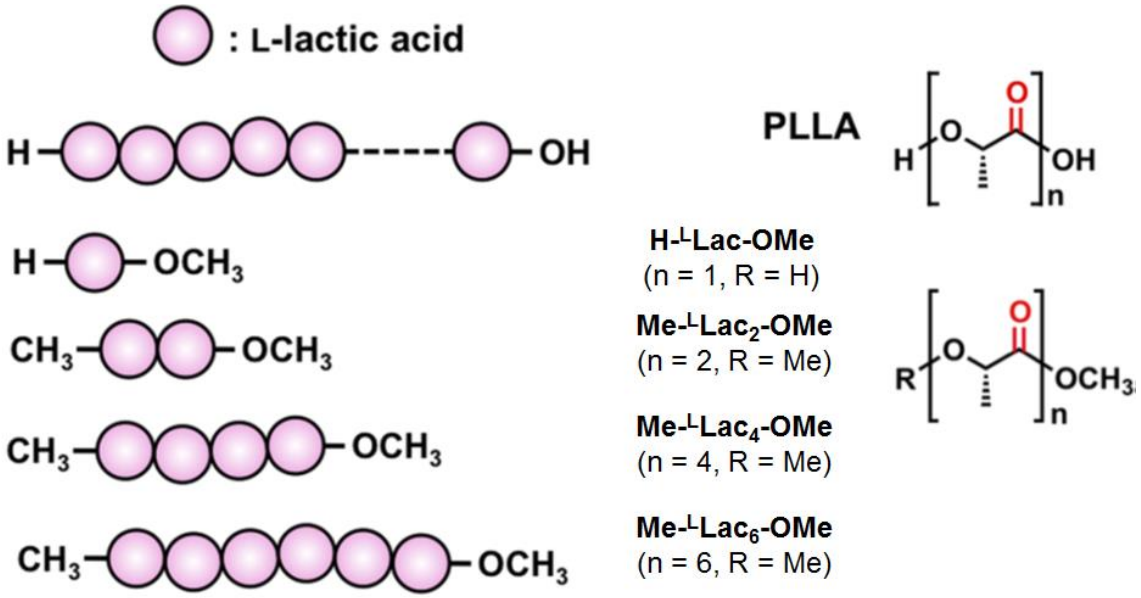

Figure 1. Schematic representation and structure of the samples usedin this study.

2-2 Results and Discussion

VCD Measurement of PLLA.

Figure 2 shows the IR and VCD spectra of PLLA in $CDCl_3$ (a) and DMSO-d_6 (b) at a concentration of 10 mg/mL. These solvents were selected for their sufficient solubility of PLLA and weak absorption in the infrared region of interest. Moreover, noncoordinating $CDCl_3$ is favored in computational VCD study owing to the high agreement between experimental spectra and theoretical ones that are calculated without considering solvent effects. On the other hand, the strongly coordinating nature of DMSO-d_6 has enabled VCD measurement of various hydrophilic biomolecules. Notwithstanding the different properties of these solvents, their experimental IR and VCD spectra were almost superimposable (Figure 2, top), which indicates that PLLA adopts almost the same conformation in these solvents at the concentration studied here. This is in contrast to other molecules whose conformation and hence VCD spectrum display solvent-dependency.[2] Importantly, these VCD spectra exhibited a strong bisignate signal in the C=O stretching region: the first negative peak at 1751 cm^{-1} and the second positive peak at 1767 cm^{-1}. On the basis of the coupled oscillator model,[3] the signs of the couplet proposed a left-handed helical structure of PLLA in which two adjacent carbonyl groups are arranged counterclockwisely (Figure 2, bottom). This conclusion is the same as that stated by Ho et al. in a recent report that recorded the VCD spectrum of PLLA for the first time.[1] On the other hand, no significant C=O stretching VCD signal was detected for monomeric Llactic acid methyl ester (H-^{L}LacOMe), whose VCD spectrum was also previously studied by Xu and co-workers,[4] at a concentration of 0.1 M (10.4 mg/mL) (Figure 1c). This observation confirmed that the observed intense VCD bands are produced by interaction of two or more carbonyl groups. These results indicated the

effectiveness of VCD spectroscopy in the solution-state structural analysis of polyester, in which carbonyl groups are abundant. Meanwhile, considering the importance of PLLA as thermoplastics, it may be interesting to study its structural analysis in a crystalline or amorphous state using VCD in future studies.

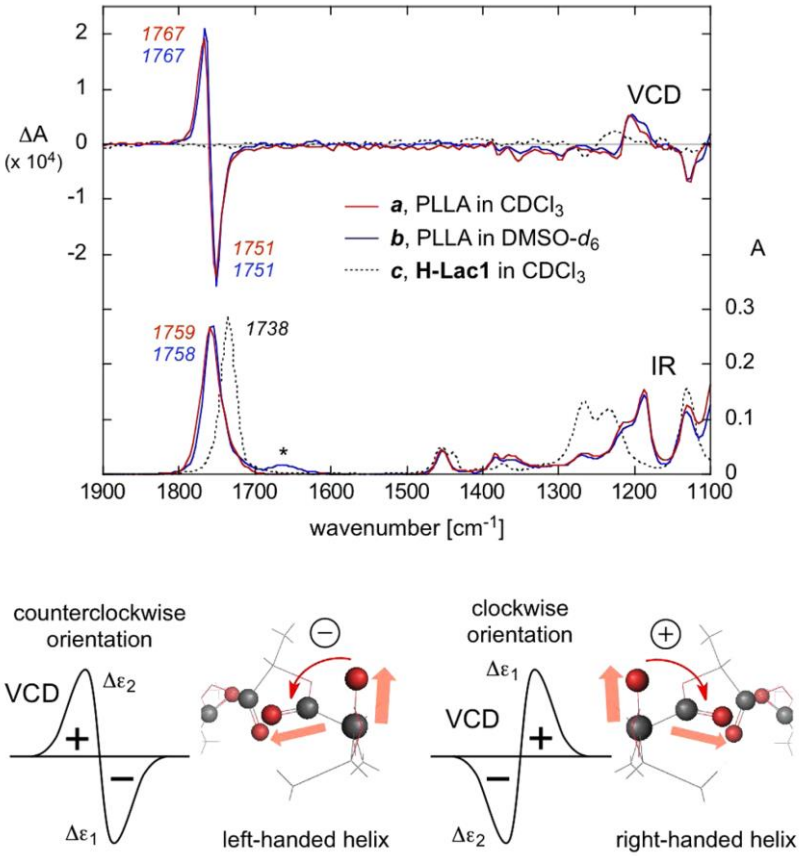

Figure 2. IR and VCD spectra of PLLA in CDCl3 and in DMSO-d6 (a and b, both at 10.0 mg/mL), and H-LacOMe in CDCl3 (c, 10.4 mg/mL, 0.1 M) (top) and the illustrative relationship between the sign of VCD couplet and the helix sense of PLA (bottom). The wavenumbers for IR and VCD peak extrema in the C=O stretching region are labeled using the same color for each sample.

VCD Measurement of Oligomers.

The observed C=O stretching VCD pattern for PLLA is reminiscent of that for PPII

helix, a left-handed 3_1 helix that exists in various proteins.[5] The PPII-like stable helical architecture of PLLA is attractive in developing a new peptidomimetic structural unit that can be, for example, incorporated into genetically engineered proteins. An embodiment of such applications requires an understanding of the structural details of short oligo(lactic acid)s in addition to those for PLA. To this end, we synthesized oligo(L-lactic acid)s **Me-^{L}Lac$_2$-OMe**, **Me-^{L}Lac$_4$-OMe**, and **Me-^{L}Lac$_6$-OMe** (Figure 1) and analyzed their vibrational spectra, first by the examination of their exciton couplet, and second by DFT calculation. This oligomer set was designed to have methyl groups both on the terminal hydroxyl group and on the carboxylic acid to mimic L-lactic acid repeating unit without affecting its exciton couplet.

Me-^{L}Lac$_2$-OMe, **Me-^{L}Lac$_4$-OMe**, and **Me-^{L}Lac$_6$-OMe** were prepared from L-lactic acid through iterative couplings using HATU (O-(7-azabenzotriazol-1-yl)-N,N,N′,N′-tetramethyluronium hexafluorophosphate), HOBt (1-hydroxybenzotriazole) and diisopropylethylamine (see Experimental Section) in order to obtain oligomers with a unified structure. The unity of each oligomer was confirmed by ^{1}H NMR measurement. The IR and VCD spectra of the oligomers in the C=O stretching region, normalized based on the integral of the C=O stretching IR band of PLLA, are shown in Figure 3. The IR absorption of each oligomer appeared as an apparent single band, justifying the choice of methyl groups to mimic L-lactic acid repeating unit. Meanwhile, unlike **H-^{L}Lac-OMe**, a negative−positive VCD pattern was observed for all oligomers. Such an exciton couplet was also observed for **Me-^{L}Lac$_2$-OMe**, suggesting that the left-handed helical tendency is already present at the level of a dimer. However, the small VCD intensity of **Me-^{L}Lac$_2$-OMe** was indicative of its conformational flexibility, as discussed later. The increase in the oligomer length brought the positions of the IR and VCD peaks and the amplitude of

the exciton couplet closer to the values for PLLA (Table 1). In particular, the relative VCD amplitude of **Me-^{L}Lac$_6$-OMe** to PLLA was 0.79 (Table 1), a value similar to an arithmetic limit based on a simplistic hypothesis where the couplet were solely generated by bischromophoric interactions of a series of pairs of adjacent carbonyl groups (i.e., since **Me-^{L}Lac$_6$-OMe** would have five bischromophoric interactions among six carbonyl groups, its relative amplitude should be ca. 0.83). Furthermore, the spectral patterns for the IR and VCD spectra of **Me-^{L}Lac$_6$-OMe** including the region below 1600 cm^{-1} are in good accord with those of PLLA (see Figure 3). These results strongly suggested that **Me-^{L}Lac$_6$-OMe** and PLLA display closely similar left-handed helical stereostructures, and therefore that detailed structural studies on **Me-^{L}Lac$_6$-OMe** should be informative in elucidating the solution-state conformation of PLLA. It should be noted that **Me-^{L}Lac$_4$-OMe** also showed a high relative VCD amplitude, 0.67 (Table 1), which is comparable to a hypothetical arithmetic limit, 0.75 (three adjacent bischromophoric pairs among four carbonyl groups). This high value indicated the strong, though not complete, lefthanded preference of **Me-^{L}Lac$_4$-OMe**. These interpretations on the basis of the intensity of VCD exciton couplet were parallel to the results of the following DFT computation.

Table 1. Comparison of the peak positions and intensities of the exciton couplet of Oligo(L-lactic acid)s and PLLA

	Me-^{L}Lac$_2$-OMe	Me-^{L}Lac$_4$-OMe	Me-^{L}Lac$_6$-OMe	PLLA
ν [cm^{-1}] at IR$_{max}$	1749	1753	1756	1759
ν [cm^{-1}] at ΔA_{1ex} [a]	1747	1747	1751	1751
ν [cm^{-1}] at ΔA_{2ex} [a]	1763	1767	1767	1767
$\int \Delta A_{1norm} d\nu$ [b]	-1.15 x 10^{-3}	-2.03 x 10^{-3}	-2.48 x 10^{-3}	-2.87 x 10^{-3} [c]
$\int \Delta A_{2norm} d\nu$ [b]	+0.71 x 10^{-3}	+1.53 x 10^{-3}	+1.72 x 10^{-3}	+2.43 x 10^{-3} [c]
amplitude of the couplet [d]	-1.86 x 10^{-3}	-3.56 x 10^{-3}	-4.20 x 10^{-3}	-5.30 x 10^{-3} [c]
relative amplitude [e]	0.35	0.67	0.79	-

[a]Wavenumber at the extrema of the first or second Cotton effect (ΔA_1 or ΔA_2, respectively). [b]Integral of the normalized first or second Cotton effect band. [c]Not normalized. [d]$\int \Delta A_{1norm}$ dν – $\int \Delta A_{2norm}$ dν. [e]Amplitude of the couplet of oligo(L-lactic acid)s relative to that of PLLA.

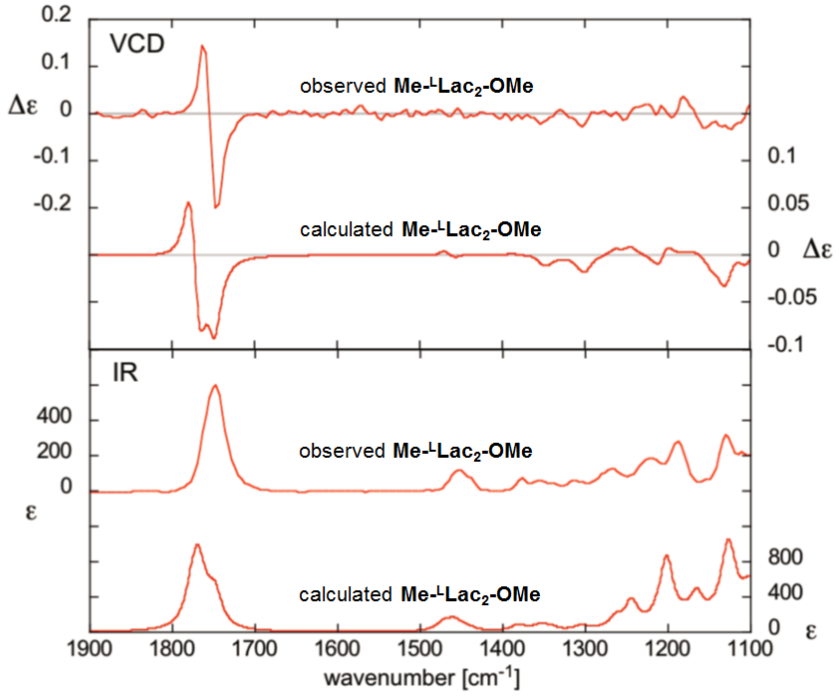

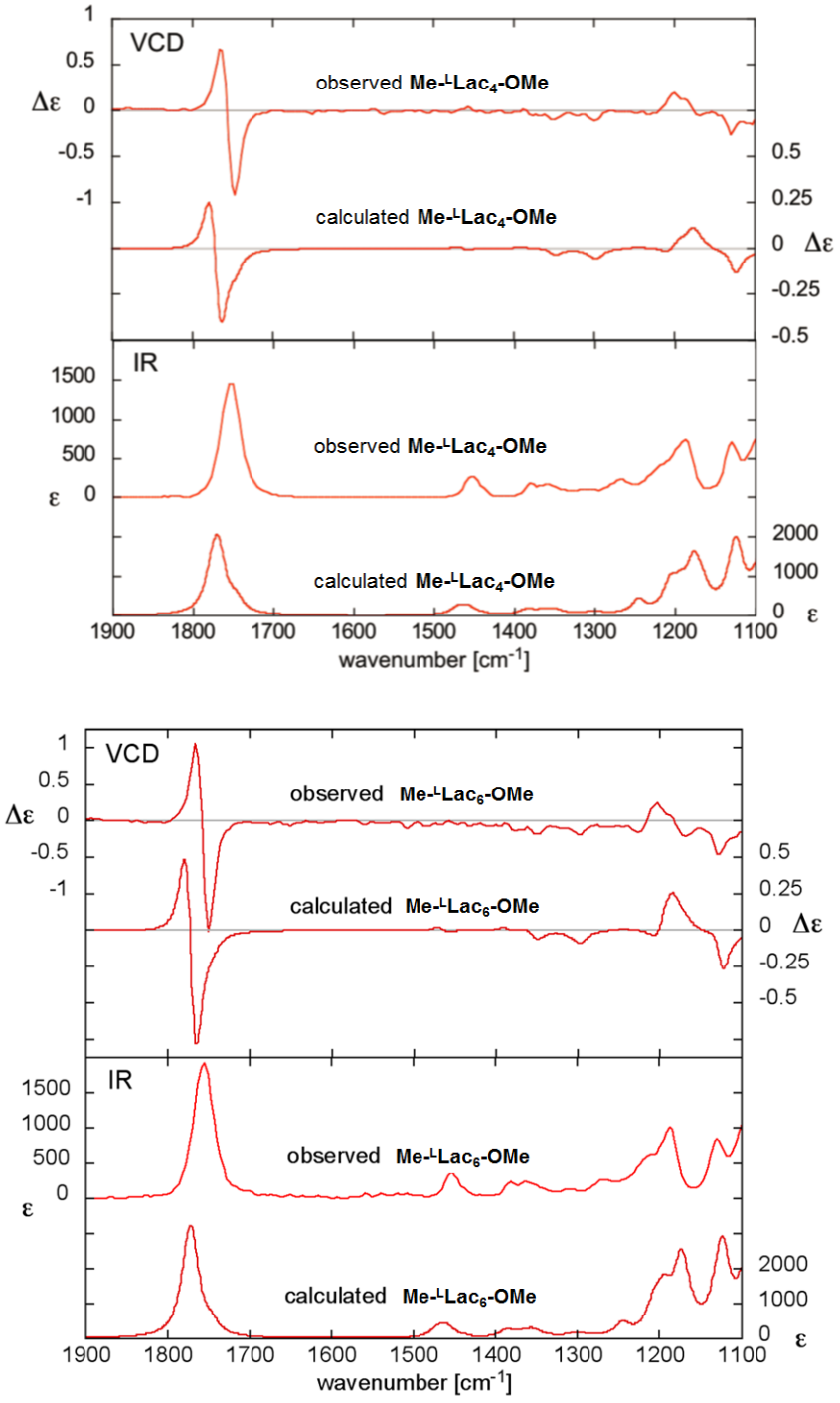

Figure 3. Comparison of observed and calculated spectra for **Me-^{L}Lac$_2$-OMe**, **Me-^{L}Lac$_4$-OMe**, and **Me-^{L}Lac$_6$-OMe**.

Detailed Structural Analysis by Density Functional Theory Calculation.

Structural studies of crystalline PLA have revealed that it displays a left-handed 10_3 helix in an α-crystalline form, and left-handed 3_1 helices in β- and γ-forms.[6,7] The conformation in a dilute solution state or a single-molecular state has been studied by theoretical calculation, for which the use of DFT has been extensive, but only a few experimental evidence have been provided to support such simulations.[8] In order to clarify the structural details of oligo(L-lactic acid)s and PLLA in a solution state, we next carried out the DFT calculations of the oligomers. Prior to the calculation of VCD spectra of **Me-^{L}Lac$_2$-OMe**, **Me-^{L}Lac$_4$-OMe**, and **Me-^{L}Lac$_6$-OMe**, geometries generated by MMFF conformational search were optimized by DFT at the B3LYP/6-311++G(d,p) level, leading to two or three conformers within 2 kcal/mol from the most stable (see Experimental Section). In our previous study, we observed the suitability of this level of theory in reproducing observed VCD exciton couplet and in predicting the conformational propensity around ester linkage: ester group prefers strans orientation, and ester carbonyl and methine hydrogen are roughly in syn relationship. Each low-energy conformer is drawn in experimental section. Table 2 lists the relative energy, Boltzmann population, rotational angles φ and ψ (C(i−1)−O(i)α−C(i) α−C(i) and O(i) α−C(i) α−C(i)−O(i+1) α, respectively, for the ith residue), and dihedral angles between two adjacent carbonyl groups of each stable conformer. All oligomers were predicted to exist mainly as two energetically close left-handed (θ = −105.1° to −108.7°) conformational states that primarily differ in the rotation around the terminal methyl ether. Additionally, a minor conformer with right-handed tendency was seen for **Me-^{L}Lac$_2$-OMe**, as expected from the weak amplitude of its VCD couplet. Meanwhile, despite the fluctuation caused by the methyl ether in our system, only left-handed species were

found for **Me-^{L}Lac$_4$-OMe** and **Me-^{L}Lac$_6$-OMe**, proposing that tetramer should be long enough to form a defined left-handed helical structure. The IR and VCD spectra of these conformers were calculated at the same level of theory, and the final spectra were obtained based on their Boltzmann population. Figure 3 shows the comparison between the experimental and the theoretical data for **Me-^{L}Lac$_6$-OMe**. While the relative intensity of the calculated IR and VCD spectra below 1250 cm^{-1}, where deformation vibrations of C−H and CH_3 groups and stretching vibrations in the backbone are dominant, is more pronounced compared to their C=O stretching regions, the sign and the shape of most of the simulated bands corresponded well with the observed. VCD simulations of **Me-^{L}Lac$_2$-OMe** and **Me-^{L}Lac$_4$-OMe** also reproduced their observed data (Figure 3). The spectral agreement bolstered the fidelity of the predicted conformers. For the first time, we demonstrated that the conformation of polyester was accurately predicted by theoretical calculation of VCD spectrum. It should be reasonable to assume that the middle part of **Me-^{L}Lac$_6$-OMe** closely reflects the microscopic conformational features of PLLA, though not long enough to describe its macromolecular behavior. As depicted in Figure 4, the carbonyl groups are aligned counterclockwisely, generating the negative−positive VCD exciton couplet. The dihedral angles of pairs of the interior carbonyl groups (θ23, θ34, and θ45) of **Me-^{L}Lac$_6$-OMe** (i) and **Me-^{L}Lac$_6$-OMe** (ii) are uniformly around −106°, a value close to that for 10_3 helix. Likewise, the rotational angles φ and ψ of second to fifth residues are around −72° and +162°, respectively, which correspond to the tg′t conformational state.[9,10] Disordered chains of PLLA in amorphous samples are suggested to contain ~80% of tg′t conformational units,[10] but our VCD results found only tg′t units within a 2 kcal/mol window in a dilute solution state. The rise per residue is approximately 3.0 Å. This value is also similar to that for reported 10_3 α-crystalline

structures (ca. 2.88 Å),[7] although the helix in solution is slightly more extended. The origin of such a secondary structure and its stability may be ascribed to steric repulsion, the aforementioned ester orientation, dipole–dipole interaction, and n → π* interaction.[11] Clarification of the degree of the contributions from each factor requires further theoretical chemistry as well as examination of various polyesters, for which VCD spectroscopy should be useful.

Table 2. Stable conformers of oligo(L-lactic acid)s calculated at DFT/B3LYP/6-311++G(d,p) level of theory.

	Me-^{L}Lac$_2$-OMe			Me-^{L}Lac$_4$-OMe		Me-^{L}Lac$_6$-OMe	
conformer	(i)	(ii)	(iii)	(i)	(ii)	(i)	(ii)
ΔE [a] [kcal/mol]	0.000	0.003	0.669	0.000	0.030	0.000	0.021
P [b] [%]	43.1	42.9	14.0	51.3	48.7	50.9	49.1
ϕ_1 [c] [deg]	-68.8	-69.4	-70.1	-69.2	-68.4	-69.2	-68.9
ψ_1 [d] [deg]	-30.2	+161.7	+165.0	+160.7	-30.3	+161.0	-28.6
ϕ_2 [d] [deg]	-73.9	-72.3	-72.6	-71.4	-72.9	-71.4	-72.4
ψ_2 [d] [deg]	+165.6	+164.7	-14.0	+160.1	+163.7	+160.4	+163.1
ϕ_3 [d] [deg]				-72.3	-70.9	-73.9	-71.4
ψ_3 [d] [deg]				+161.6	+160.5	+161.5	+161.7
ϕ_4 [d] [deg]				-74.3	-74.6	-72.9	-72.7
ψ_4 [d] [deg]				+167.3	+167.7	+166.1	+164.6
ϕ_5 [d] [deg]						-70.1	-71.7
ψ_5 [d] [deg]						+160.7	+161.9
ϕ_6 [d] [deg]						-73.8	-73.6
ψ_6 [e] [deg]						+166.8	+166.7
θ_{12} [f] [deg]	-106.6	-107.4	+24.3	-108.7	-106.8	-108.6	-106.8
θ_{23} [f] [deg]				-107.1	-106.8	-106.2	-106.1
θ_{34} [f] [deg]				-105.8	-105.5	-105.1	-105.5
θ_{45} [f] [deg]						-105.7	-106.0
θ_{56} [f] [deg]						-105.3	-105.4

[a]Relative energy. [b]Boltzmann population at 298 K. [c]Dihedral angle C_{Me}–Oα–Cα–C. [d]ϕ = dihedral angle of C(i–1)–O(i)α–C(i)α–C(i), ψ =dihedral angle of O(i)α–C(i)α–C(i)–O(i+1)α, for ith residue. [e]Dihedral angle Oα–Cα–C–O_{Me}. [f]Dihedral angle between ith and (i+1)th carbonyl groups.

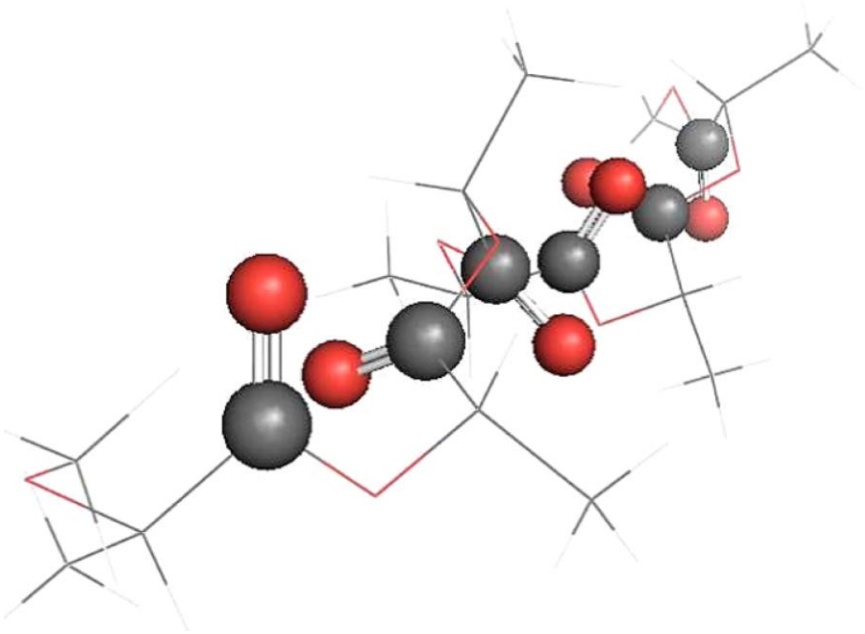

Figure 4. Orientation of the carbonyl groups of **Me-^{L}Lac$_6$-OMe(i)**

2-3 Conclusions

This study has revealed the in-depth structural nature of PLA in a solution state. PLA was found to feature a left-handed helix that was quite stable that no major influence from solvents and host molecules was observed. Furthermore, such a helical structure is formed even for short oligomers. The information obtained here should be beneficial for future applications of oligo(L-lactic acid)s as a rigid structural unit for genetically engineered proteins.

2-4 Experimental Sction

Materials.

PLLA (Mw = ~60 000) and **H-^{L}Lac-OMe** were purchased from Aldrich and TCI Fine Chemicals, respectively, and used without further purification. Oligo(lactic acid)s **Me-^{L}Lac$_2$-OMe**, **Me-^{L}Lac$_4$-OMe**, and **Me-^{L}Lac$_6$-OMe** were chemically synthesized as described in Supporting Information. Spectroscopic grade solvents were used for VCD measurements. Preparation of the DMSO-d_6 solution of PLLA required heating of the solution at ~70 °C for 5 min.

Spectral Measurements.

IR and VCD spectra were measured for 2 and 90 min, respectively, using a BioTools Chiral*ir* equipped with a second photoelastic modulator. All spectra were recorded using a 100-μm CaF_2 cell at a resolution of ca. 8 cm^{-1} at ambient temperature. All spectral data were corrected by a solvent spectrum obtained under the identical experimental condition. IR absorption maxima were determined by a JASCO FT/IR-470 spectrometer at a resolution of 1 cm^{-1}. The concentrations of oligo(L-lactic acid)s were defined as 0.1 M per carbonyl group. The IR and VCD data of PLLA-amylose complex in Figure 4 and oligo(L-lactic acid)s in Figure 5 were normalized based on the area of the carbonyl stretching IR band of PLLA in DMSO-d_6 and $CDCl_3$, respectively. Normalization on the basis of the intensity of the IR peak maxima afforded qualitatively similar results.

Computational Details.

A preliminary MMFF conformational search was performed on SPARTAN'10 software.[40] The resultant conformers within 10 kcal/mol from the most stable of each molecule were

optimized at the DFT/B3LYP/6-311++G(d,p) level, as implemented on Gaussian 09 package.[41] For **Me-^{L}Lac$_6$-OMe**, the resultant 10_3-like stable conformers were manually modified to 3_1 left-handed helix, and then submitted to DFT structural optimization, which resulted in the reproduction of the initial 10_3-like conformers. The IR and VCD spectra were calculated for the stable conformers within a 2.0 kcal/mol window at the same level of theory with Lorentzian lineshapes of 10 cm^{-1} width, and the final spectra were obtained based on the Boltzmann population average of each conformer. The calculated frequencies were scaled by a factor of 0.98.

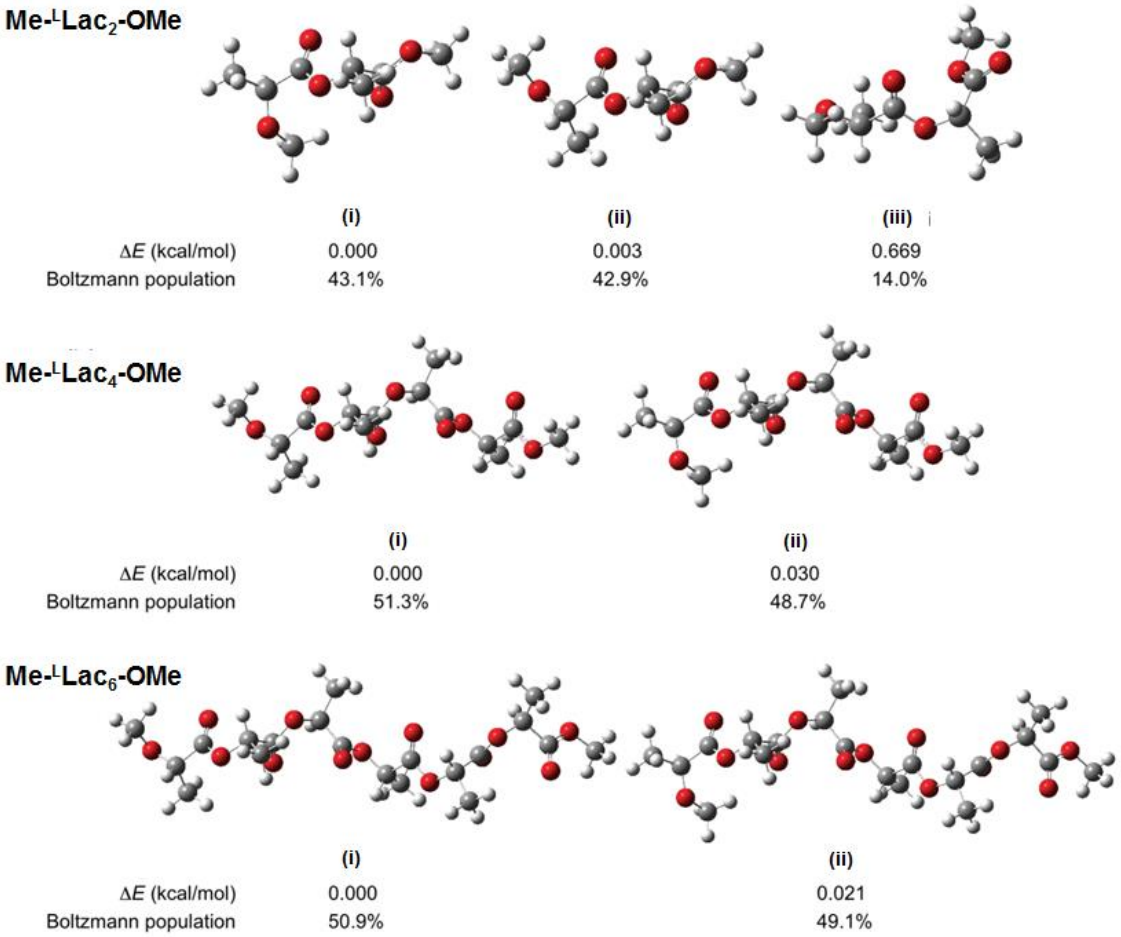

Figure S1. Stable conformers of oligo(L-lactic acid)s predicted at DFT/B3LYP/6-311++G(d,p) level of theory. Boltzmann populations were calculated at 298K.

Synthetic Procedures

^{1}H (500 MHz) and ^{13}C NMR (125 MHz) spectra were recorded on a Varian Inova instrument at 25 °C in $CDCl_3$. Chemical shifts (δ) are reported in ppm relative to $CDCl_3$ (^{1}H, δ 7.26; ^{13}C, δ 77.00), CD_3OD (^{1}H, δ 4.87; ^{13}C, δ 49.15) or tetramethylsilane. The following abbreviations were used for signal multiplicities: s = singlet; d = doublet; t = triplet; q = quadruplet; m = multiplet. Electrospray ionization mass spectra were obtained by a JEOL JMS-T100LP spectrometer or by a Thermo Scientific Exactive spectrometer. Optical rotations were measured on a JASCO P-1020 polarimeter at the sodium D-line using a 1-cm optical cell under ambient temperature, and reported as $[\alpha]_D$ (concentration in grams/100 mL solvent). TLC was performed on 0.2 mm silica gel plates (Merck 60 F254), and column chromatography was carried out on silica gel (Kanto60N, 40-50 μm). Spectroscopic grade chloroform was purchased from Wako Pure Chemical Industries, Ltd., and $CDCl_3$ and DMSO-d_6 were purchased from Cambridge Isotope Laboratories. L-Lactic acid was purchased from Wako Pure Chemical Industries, Ltd

.

(a) General procedure for ester coupling

To a stirred solution of a carboxyl acid compound and an alcohol compound in dry CH_2Cl_2 (5 mL/mmol) and dry DMF (1.7 mL/mmol), 1.1-1.6 equiv of HATU, HOBt, and DIPEA were added. After 3 to 24 h, the mixture was diluted with EtOAc, washed sequentially with 10% citric acid aq, sat $NaHCO_3$ aq, and sat NaCl aq, and then dried over $MgSO_4$. After removal of the solvent under reduced pressure, the crude mixture was purified by column chromatography (hexane/EtOAc solvent system).

(b) General procedure for removal of benzyl protecting group

A THF solution (6.0 mL/mmol) of a benzylated compound and a catalytic amount of 10% Pd/C was stirred under H_2 atmosphere at room temperature. After 2 to 3 h, the mixture was diluted with EtOAc, filtered through Celite to remove Pd/C. Removal of the solvent from the filtrate under reduced pressure yielded pure debenzylated product.

(c) General procedure for deprotection of THP protecting group

To a stirred solution of a THP-protected compound in MeOH (6.0 mL/mmol) at room temperature, 0.01-0.02 equiv of *p*-TsOH was added. After 2 h, the mixture was diluted with EtOAc, washed sequentially with sat $NaHCO_3$ aq and sat NaCl aq, and then dried over $MgSO_4$. After removal of the solvent under reduced pressure, the residue was subjected to column chromatography (hexane/EtOAc solvent system) to yield a desired deprotected product.

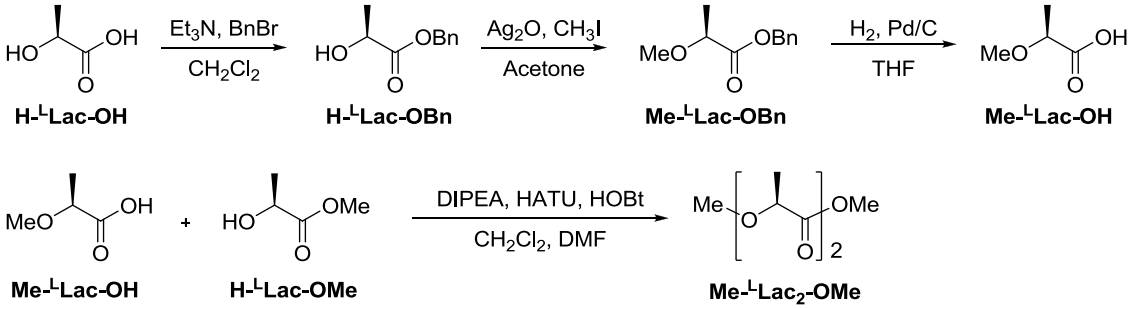

Me-^{L}Lac$_2$-OMe: L-Lactic acid (5.4 g, 60 mmol) in CH_2Cl_2 (15 mL) was added BnBr (7.12 mL, 1.0 equiv) and Et_3N (10 mL, 1.2 equiv), and then the mixture was stirred overnight at rt. The mixture was diluted with EtOAc, washed sequentially with 10% citric acid aq, sat $NaHCO_3$ aq and sat NaCl aq, and then dried over $MgSO_4$. After removal of the solvent, the residue was purified by column chromatography (hexane:EtOAc = 7:1 to 6:1)

affording **H-^{L}Lac-OBn** (6.5 g, 60%). The NMR spectrum was identical with that reported in ref 1.

H-^{L}Lac-OBn (540 mg, 3.0 mmol) in acetone (3 mL) was added MeI (1.86 mL, 10 equiv) and Ag_2O (869 mg, 1.5 equiv), and the mixture was stirred overnight at rt. The mixture was diluted with EtOAc, filtered to remove Ag_2O, washed sequentially with water and brine, and then dried over $MgSO_4$. After removal of the solvent, the residue was subjected to column chromatography (hexane:EtOAc = 7:1 to 6:1), affording **Me-^{L}Lac-OBn** (332 mg, 57%): ^{1}H NMR ($CDCl_3$) δ 7.38-7.31 (m, 5H, ArH), 5.21 (d, *J* = 12.2 Hz, 1H, Ph$\underline{CH_2}$), 5.19 (d, *J* = 12.3 Hz, 1H, Ph$\underline{CH_2}$), 3.92 (q, *J* = 6.3 Hz, 1H, Hα), 3.39 (s, 3H, CH_3O), 1.42 (d, *J* = 6.8 Hz, 3H, CH_3); ^{13}C NMR ($CDCl_3$) δ 172.95 (C=O), 135.62, 128.58, 128.35, 128.21 (each Ar), 76.38 (Cα), 66.51 (Ph$\underline{CH_2}$), 57.72 (CH_3O), 18.41 (CH_3); $[\alpha]_D$ -27.9 (c 0.1, $CHCl_3$).

Following the general procedure (b), **Me-^{L}Lac-OBn** (320 mg, 1.64 mmol) was converted to **Me-^{L}Lac-OH** (171 mg, q.y.). The NMR spectrum was identical with that reported in ref 3.

Following the general procedure (a), **Me-^{L}Lac-OH** (31 mg, 0.30 mmol) and **H-^{L}Lac-OMe** (31 mg 0.30 mmol) were coupled to produce **Me-^{L}Lac$_2$-OMe** (30 mg 53%): ^{1}H NMR ($CDCl_3$) δ 5.20 (q, *J* =7.2 Hz, 1H, Hα), 3.96 (q, *J* = 6.8 Hz, 1H, Hα), 3.76 (s, 3H, CH_3O), 3.44 (s, 3H, CH_3O), 1.54 (d, *J* = 7.1 Hz, 3H, CH_3), 1.47 (d, *J* = 6.8 Hz, 3H, CH_3); ^{13}C NMR ($CDCl_3$) δ 172.61, 170.85 (C=O), 76.18, 68.65, (Cα), 57.73 (CH_3O), 52.36 (OCH_3), 18.41, 16.90 (CH_3); HRMS (ESI) m/z calcd for $C_8H_{14}O_5Na$ $[M+Na]^+$ 213.0733, found 213.0736; $[\alpha]_D$ -34.1 (c 0.1, $CHCl_3$).

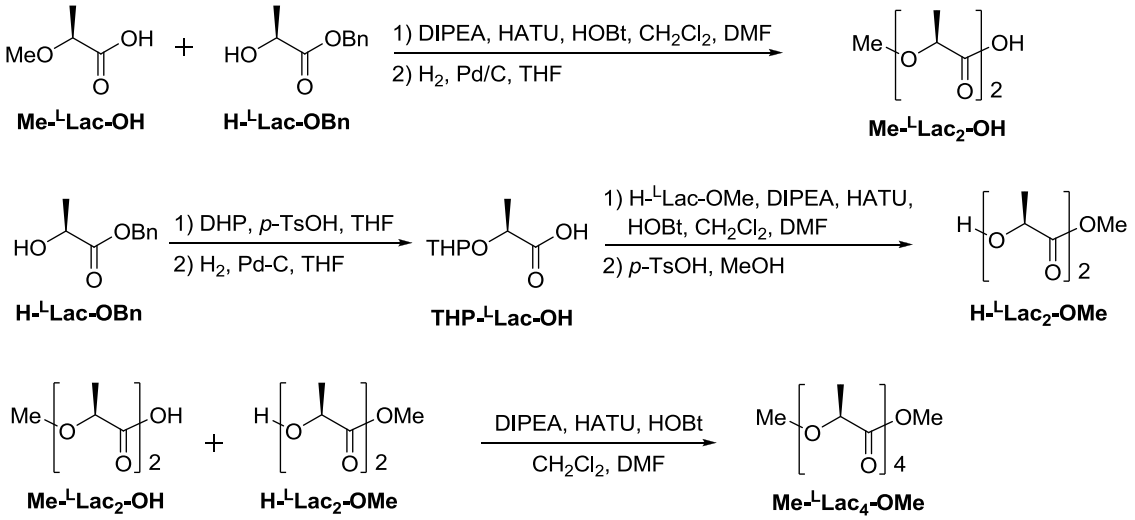

Me-^{L}Lac$_4$-OMe: Following the general procedure (a), **Me-^{L}Lac-OH** (62 mg, 0.6 mmol) and **H-^{L}Lac-OBn** (108 mg 0.6 mmol) were coupled to produce **Me-^{L}Lac$_2$-OBn** (147 mg, 92%): ^{1}H NMR ($CDCl_3$) δ 7.40-7.31 (m, 5H, ArH), 5.23 (q, J = 7.3 Hz, 1H, Hα), 5.20 (d, J = 12.7 Hz, 1H, Ph$\underline{CH_2}$), 5.16 (d, J = 12.3 Hz, 1H, Ph$\underline{CH_2}$), 3.93 (q, J = 7.0 Hz, 1H, Hα), 3.40 (s, 3H, CH_3O), 1.55 (d, J = 7.0 Hz, 3H, CH_3), 1.41 (d, J = 7.0 Hz, 3H, CH_3); ^{13}C NMR ($CDCl_3$) δ 172.95, 170.21 (C=O), 135.13, 128.60, 128.47, 128.25 (each Ph), 76.16, 68.74 (Cα), 67.15 (Ph$\underline{CH_2}$), 57.73 (CH_3O), 18.41, 16.88 (CH_3); LRMS (ESI) m/z calcd for $C_{14}H_{18}O_5Na$ $[M+Na]^+$ 289.1, found 289.2; $[\alpha]_D$ -55.0 (c 0.1, $CHCl_3$).

Following the general procedure (b), **Me-^{L}Lac$_2$-OBn** (135 mg, 0.51 mmol) was converted to **Me-^{L}Lac$_2$-OH** (89 mg, q.y.): ^{1}H NMR (CD_3OD) δ 5.10 (q, J = 6.9 Hz, 1H, Hα), 3.93 (q, J = 6.7 Hz, 1H, Hα), 3.39 (s, 3H, CH_3O), 1.51 (d, J = 6.9 Hz, 3H, CH_3), 1.40 (d, J = 6.8 Hz, 3H, CH_3); ^{13}C NMR (CD_3OD) δ 172.84, 172.27 (C=O), 75.87, 68.78, (Cα), 56.57 (CH_3O), 17.30, 15.80 (CH_3); HRMS (ESI) m/z calcd for $C_7H_{11}O_5$ $[M-H]^-$ 175.0612, found 175.0610; $[\alpha]_D$ -78.3 (c 0.1, $CHCl_3$).

H-^{L}Lac-OBn (1.80 g, 10.0 mmol) in THF (6 mL) was added 3,4-dihydro-2H-pyran (1.1 mL, 1.3 equiv) and *p*-TsOH (19 mg, 0.01 equiv), and then the mixture was stirred

overnight at rt. The mixture was diluted with EtOAc, washed sequentially with sat $NaHCO_3$ aq and sat NaCl aq, and then S7 dried over $MgSO_4$. After removal of the solvent, the residue was subjected to column chromatography (hexane:EtOAc = 10:1), affording a diastereomeric mixture of **THP-^{L}Lac-OBn** (2.47 g, 94%, dr 0.67:0.33): ^{1}H NMR ($CDCl_3$) δ 7.39-7.30 (m, 5H, ArH), 5.18 (d, *J* = 12.3Hz, 2H, Ph$\underline{CH_2}$), 4.72 (t, *J* = 3.4 Hz, 0.33H, OCHO), 4.70 (t, *J* = 3.8 Hz, 0.67H, OCHO), 4.47 (q, *J* = 7.0 Hz, 0.67H, Hα), 4.27 (q, *J* = 6.9 Hz, 0.33H, Hα), 3.91-3.81 (m, 1H, OCH_2-), 3.54-3.47 (m, 0.67H, OCH_2), 3.41-3.35 (m, 0.33H, OCH_2), 1.91-1.80 (m, 1H, -CH_2-), 1.79-1.63 (m, 2H, -CH_2-) , 1.62-1.49 (m, 3H, -CH_2-), 1.49 (d, *J* = 6.9 Hz, 2H, CH_3), 1.41 (d, *J* = 6.9 Hz, 1H, CH_3).

Following the general procedure (b), **THP-^{L}Lac-OBn** (2.47 g, 9.33 mmol) was converted to **THP-^{L}Lac-OH** (1.49 g, 92%). The NMR spectrum was identical with that reported in ref 4.

Following the general procedure (a), **THP-^{L}Lac-OH** (89 mg, 0.5 mmol) and **H-^{L}Lac-OMe** (52 mg 0.5 mmol) were coupled to produce **THP-^{L}Lac$_2$-OMe**, which was directly converted to **H-^{L}Lac$_2$-OMe** (27 mg, 15% in 2 steps) following the general procedure (c). The NMR spectrum of **H-^{L}Lac$_2$-OMe** was identical with that reported in ref 5.

Following the general procedure (a), **Me-^{L}Lac$_2$-OH** (24 mg, 0.085 mmol) and **H-^{L}Lac$_2$-OMe** (24 mg 0.085 mmol) were coupled to produce **Me-^{L}Lac$_4$-OMe** (27 mg, 60%): ^{1}H NMR ($CDCl_3$) δ 5.23-5.12 (m, 3H, Hα), 3.95 (q, J = 6.7 Hz, 1H, Hα), 3.74 (s, 3H, OCH_3), 3.42 (s, 3H, CH_3O), 1.60 (m, 6H, CH_3), 1.51 (d, *J* = 7.1 Hz, 3H, CH_3), 1.45 (d, *J* = 7.1 Hz, 3H, CH_3); ^{13}C NMR ($CDCl_3$) δ 172.65, 170.54, 169.88, 169.62 (C=O), 76.11, 69.17, 68.96, 68.46 (Cα), 57.78 (CH_3O), 52.40 (OCH_3), 18.44, 16.77, 16.74, 16.44 (CH_3); LRMS (ESI) m/z calcd for $C_{14}H_{22}O_9Na$ $[M+Na]^+$ 357.1, found 357.2; $[\alpha]_D$ -88.6 (c 0.1, $CHCl_3$).

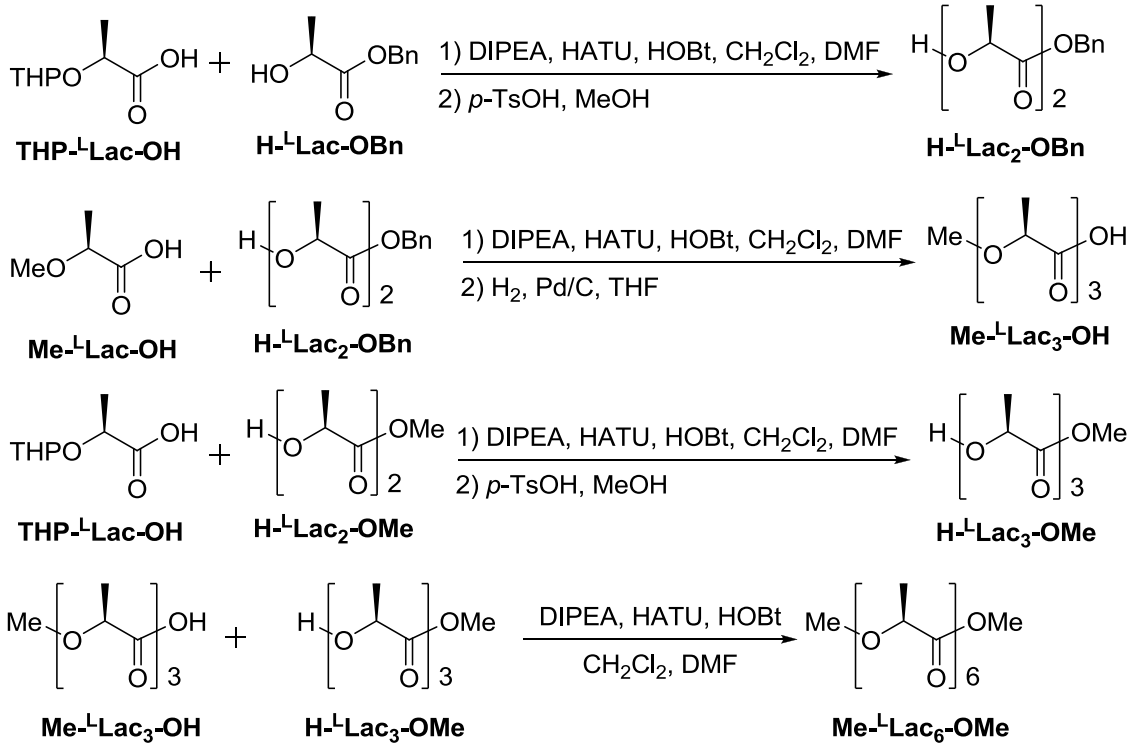

Me-^{L}Lac$_6$-OMe: Following the general procedure (a), **THP-^{L}Lac-OBn** (524 mg, 3.0 mmol) and **H-^{L}Lac-OBn** (545 mg 3.0 mmol) were coupled to produce **THP-^{L}Lac$_2$-OBn** (740 mg, 81%). Following the general procedure (c), **THP-^{L}Lac$_2$-OBn** (740 mg, 2.24 mmol) was converted to **H-^{L}Lac$_2$-OBn** (444 mg 78%). The NMR spectrum of S6 was identical with that reported in ref 6.

Following the general procedure (a), **Me-^{L}Lac-OH** (112 mg, 1.15 mmol) and **H-^{L}Lac$_2$-OBn** (291 mg 1.15 mmol) were coupled to produce **Me-^{L}-Lac$_3$-OBn** (201 mg, 52%): ^{1}H NMR ($CDCl_3$) δ 7.39-7.31 (m, 5H, ArH), 5.21 (q, J = 6.9 Hz, 1H, Hα), 5.20 (q, J = 6.9 Hz, 1H, Hα), 5.20 (d, J = 12.4 Hz, 1H, Ph$\underline{CH_2}$), 5.14 (d, J = 12.4 Hz, 1H, Ph$\underline{CH_2}$), 3.95 (q, J = 7.0 Hz, 1H, Hα), 3.43 (s, 3H, CH_3O), 1.55 (d, J = 7.9 Hz, 3H, CH_3), 1.53 (d, J = 5.9 Hz, 3H, CH_3), 1.46 (d, J = 6.9 Hz, 3H, CH_3); ^{13}C NMR ($CDCl_3$) δ 172.65, 169.97, 169.83 (C=O),

135.09, 128.60, 128.48, 128.23 (each Ph), 76.13, 69.20, 68.47, (Cα), 67.18 (Ph$\underline{CH_2}$), 57.77 (CH_3O), 18.44, 16.78, 16.69 (CH_3); LRMS (ESI) m/z calcd for $C_{17}H_{22}O_7Na$ $[M+Na]^+$ 361.1, found 361.2; $[\alpha]_D$ -72.8 (c 0.1, $CHCl_3$).

Following the general procedure (b), **Me-^{L}-Lac$_3$-OBn** (194 mg, 0.57 mmol) was converted to **Me-^{L}-Lac$_3$-OH** (143 mg, q.y.): ^{1} H NMR (CD_3OD) δ 5.19 (q, *J* = 7.0 Hz, 1H, Hα), 5.08 (q, *J* = 7.2 Hz, 1H, Hα), 3.98 (q, *J* = 6.5 Hz, 1H, Hα), 3.38 (s, 3H, CH_3O), 1.56 (d, *J* = 6.9 Hz, 3H, CH_3), S9 1.50 (d, *J* = 7.0 Hz, 3H, CH_3), 1.40 (d, *J* = 6.9 Hz, 3H, CH_3); ^{13}C NMR (CD_3OD) δ 172.74, 172.13, 169.97 (C=O), 75.80, 69.28, 68.63 (Cα), 56.59 (CH_3O), 17.34, 15.78, 15.59 (CH_3); LRMS (ESI) m/z calcd for $C_{10}H_{16}O_7Na$ $[M+Na]^+$ 271.1, found 271.1; $[\alpha]_D$ -83.3 (c 0.1, $CHCl_3$).

Following the general procedure (a), **THP-^{L}Lac-OH** (30 mg, 0.17 mmol) and **H-^{L}Lac$_2$-OMe** (25 mg 0.14 mmol) were coupled to produce a diastereomeric mixture of **THP-^{L}Lac$_3$-OMe**, which was directly converted to **H-^{L}Lac$_3$-OMe** (11 mg, 20% in 2 steps) following the general procedure (c): ^{1}H NMR ($CDCl_3$) δ 5.22 (q, *J* = 7.1 Hz, 1H, Hα), 5.17 (q, *J* = 7.0 Hz, 1H, Hα), 4.36 (q, *J* = 7.0 Hz, 1H, Hα), 3.75 (s, 3H, OCH_3), 1.61 (d, *J* = 7.0 Hz, 3H, CH_3), 1.53 (d, *J* = 7.0 Hz, 3H, CH_3), 1.50 (d, *J* = 7.0 Hz, 3H, CH_3); ^{13}C NMR ($CDCl_3$) δ 175.14, 170.51, 169.59 (C=O), 69.22, 69.15, 66.70 (Cα), 52.44 (OCH_3), 20.50, 16.80, 16.70 (CH_3); LRMS (ESI) m/z calcd for $C_{10}H_{16}O_7Na$ $[M+Na]^+$ 271.1, found 271.2; $[\alpha]_D$ -56.0 (c 0.1, $CHCl_3$).

Following the general procedure (a), **Me-^{L}-Lac$_3$-OH** (11 mg, 0.044 mmol) and **H-^{L}Lac$_3$-OMe** (11 mg 0.044 mmol) were coupled to produce **Me-^{L}Lac$_6$-OMe** (13 mg 62%): ^{1}H NMR ($CDCl_3$) δ 5.23-5.13 (m, 5H, Hα), 3.95 (q, *J* = 6.9 Hz, 1H, Hα), 3.74 (s, 3H, OCH_3), 3.43 (s, 3H, CH_3O), 1.61-1.58 (m, 12H, CH_3), 1.51 (d, *J* = 7.0 Hz, 3H, CH_3), 1.45 (d, *J* = 6.9 Hz, 3H, CH_3); ^{13}C NMR ($CDCl_3$): δ 172.67, 170.54, 169.91, 169.67, 169.62, 169.58 (C=O),

76.14, 69.20, 69.04, 69.00, 68.94, 68.47 (Cα), 57.79 (CH_3O), 52.44 (OCH_3), 18.47, 16.79, 16.77, 16.69, 16.65, 16.62 (CH_3); LRMS (ESI) m/z calcd for $C_{20}H_{30}O_{13}Na$ $[M+Na]^+$ 501.2, found 501.3; $[\alpha]_D$ -99.0 (c 0.1, $CHCl_3$).

2-5 References

1 Ho, R.-M.; Li, M.-C.; Lin, S.-C.; Wang, H.-F.; Lee, Y.-D.; Hasegawa, H.; Thomas, E. L. *J. Am. Chem. Soc.* **2012**, *134*, 10974−10986.

2 (a) Tang, H.-Z.; Novak, B. M.; He, J.; Polavarapu, P. L. *Angew. Chem., Int. Ed.* **2005**, *44*, 7298−7301. (b) Abbate, S.; Lebon, F.; Longhi, G.; Boiadjiev, S. E.; Lightner, D. A. *J. Phys. Chem. B* **2012**, *116*, 5628−5636. (c) Zhang, P.; Polavarapu, P. L. *J. Phys. Chem. A* **2007**, *111*, 858−871.

3 (a) Tinoco, I. *Radiat. Res.* ***1963***, *20*, 133−139. (b) Freedman, T. B.; Nafie, L. A. *Top. Stereochem.* ***1987***, *17*, 113−206. (c) Abbate, S.; Gangemi, R.; Longhi, G. *J. Chem. Phys.* ***2002***, *117*, 7575−7586.

4 (a) Losada, M.; Xu, Y. *Phys. Chem. Chem. Phys.* ***2007***, *9*, 3127−3135. (b) Losada, M.; Tran, H.; Xu, Y. *J. Chem. Phys.* ***2008***, *128*, 014508. (c) Liu, Y.; Yang, G.; Losada, M.; Xu, Y. *J. Chem. Phys.* ***2010***, *132*, 234513.

5 (a) Dukor, R. K.; Keiderling, T. A. *Biopolymers* ***1991***, *31*, 1747−1761. (b) Taniguchi, T.; Monde, K. *Chem. -Asian J.* ***2007***, *2*, 1258−1266. (c) Bochicchio, B.; Tamburro, A. M. *Chirality* ***2002***, *14*, 782−792.

6 (a) Jiang, X.; Luo, Y.; Tian, X.; Huang, D.; Reddy, N.; Yang, Y. *Chemical Structure of Poly(lactic acid). In Poly(lactic acid): Synthesis, Structures, Properties, Processing, and Applications*; Auras, R. A., Lim, L.-T., Selke, S. E. M., Tsuji, H., Eds.; John Wiley & Sons: Hoboken, NJ, 2010; p 69. (b) Irsai, I.; Majdik, C.; Lupan, A.; Silaghi-Dumitrescu, R. *J. Math. Chem.* ***2012***, *50*, 703−733.

7 (a) Hoogsteen, W.; Postema, A. R.; Pennings, A. J.; ten Brinke, G.; Zugenmaier, P. *Macromolecules* ***1990***, *23*, 634−642. (b) Sasaki, S.; Asakura, T. *Macromolecules* ***2003***, *36*, 8385−8390. (c) Wasanasuk, K.; Tashiro, K.; Hanesaka, M.; Ohhara, T.; Kurihara, K.;

Kuroki, R.; Tamada, T.; Ozeki, T.; Kanamoto, T. *Macromolecules* **2011**, *44*, 6441−6452.

8 (a) Jarmelo, S.; Marques, D. A. S.; Simões, P. N.; Carvalho, R. A.; Batista, C. M. S. G.; Araujo-Andrade, C.; Gil, M. H.; Fausto, R. *J. Phys. Chem. B* **2012**, *116*, 9−21. (b) Casalini, T.; Rossi, F.; Santoro, M.; Perale, G. Int. *J. Mol. Sci.* **2011**, *12*, 3857−3870.

9 (a) Kang, S.; Hsu, S. L.; Stidham, H. D.; Smith, P. B.; Leugers, M. A.; Yang, X. *Macromolecules* **2001**, *34*, 4542−4548. (b) Yang, X.; Kang, S.; Hsu, S. L.; Stidham, H. D.; Smith, P. B.; Leugers, A. *Macromolecules* **2001**, *34*, 5037−5041.

10 (a) Yang, X.; Kang, S.; Yang, Y.; Aou, K.; Hsu, S. L. *Polymer* **2004**, *45*, 4241−4248. (b) Rathi, S.; Kalish, J. P.; Coughlin, E. B.; Hsu, S. L. *Macromolecules* **2011**, *44*, 3410−3415.

11 (a) Newberry, R. W.; Raines, R. T. *Chem. Commun*. **2013**, *49*, 7699−7701. (b) Bartlett, G. J.; Choudhary, A.; Raines, R. T.; Woolfson, D. N. *Nat. Chem. Biol.* **2010**, *6*, 615−620.

12 Stayshich, R. M.; Meyer, T. Y. *J. Am. Chem. Soc.* **2010**, *132*, 10920-10934.

13 Davies, S. G.; Wills, M. *J. Organomet. Chem.* **1987**, *328*, C29-C33.

14 Barrett, A. G. M.; Braddock, D. C.; Christian, P. W. N.; Pilipauskas, D.; White, A. J. P.; Williams, D. J. *J. Org. Chem.* **1998**, *63*, 5818-5823.

15 Kuisle, O.; Quiñoá, E.; Riguera, R. *J. Org. Chem.* **1999**, *64*, 8063-8075.

16 Phomphrai, K.; Pracha, S.; Phonjanthuek, P.; Pohmakotr, M. *Dalton Trans.* **2008**, 3048-3050.

17 Zhu, H.; Xu, X.; Cui, W.; Zhang, Y.; Mo, H.; Shen, Y.-M. *J. Polym. Sci. A Polym. Chem.* **2011**, *49*, 1745-1752.

Chapter 3

Controlling Oligoalanine Conformation by Replacement of Amide to Ester Linkage

3-1 Introduction

As described in Chapter 1, PPII helix is a left-handed 3_1-helix found in various proteins such as collagen, elastin, and casein.[1,2] PPII helix does not form intramolecular hydrogen bonds, unlike right-handed α-helix, which forms hydrogen bonds between the C=O group of the *i*th residue and the NH group of the (*i*+4)th residue. As a result, PPII adopts a rather extended structure and its carbonyl and amino groups are readily accessible by other molecules for intermolecular interactions. These structural properties have rendered PPII numerous possibilities as functional motifs for protein-protein interactions, molecular scaffold, peptide-based drugs, antifreeze agent, and so on.[3-6] However, designing a peptide sequence forming a PPII helix without proline residues is sometimes difficult because of the lack of stabilizing hydrogen bonds. For example, oligoalanines may adopt multiconformational states including not only PPII[7-9] but also α-helix,[10,11] β-strand and the resultant self-assembled fibrils.[12,13] As another example, we have witnessed that antifreeze glycopeptide (AFGP) H-[Ala-Thr-Ala]$_n$-OH exists as PPII when its Thr residues are glycosylated with *N*-acetylgalactosamine, while it shows an electronic circular dichroism (ECD) spectrum typical for disordered structures when it is unglycosylated.[14,15] A method to facilitate the formation of PPII helix should benefit medicinal chemistry and biochemistry using peptides and their analogues.

Modification of amide linkages in the peptide main chain to different ones (e.g. urea, carbamate, and aminoxy) has been effective in regulating their secondary structures and hence their functions.[16,17] Considering future applications to biological systems, ester linkage is promising because of (1) low toxicity, (2) easy availability (e.g. solid-phase synthesis using α-hydroxy acids, genetic code expansion, etc.),[18-20] and (3) ability to alter polypeptide conformation due to the impaired hydrogen bonding property.[18,21]

Among many α-hydroxy acids, lactic acid (Lac) is often incorporated into oligopeptides: for example, a recent study found that substitution of an Ala residue to Lac changed the conformations of pentapeptides and heptapeptides from the 11-helix to the 14/15-helix.[21] Meanwhile, to the best of our knowledge, there has been no study on the conformations of oligopeptides containing di- and longer oligo(lactic acid)s. Recently, the solution conformation of poly(L-lactic acid), a biodegradable thermoplastic polyester, was studied by Ho's and our groups by means of VCD spectroscopy.[22,23] A negative-positive VCD couplet at around 1760 cm^{-1} observed under several conditions suggested that poly(L-lactic acid) adopt a fairly stable left-handed 10_3-like helix in solution,[23-25] unlike multiconformational oligoalanines. Moreover, conformational studies on several oligo(L-lactic acid)s indicated that four ester linkages is sufficient to fix their helicity.[23] These results inspired us to use oligo(L-lactic acid) sequences as a rigid structural unit for ester-containing peptides.

In this current work, we prepared several hexamers composed of oligo(lactic acid) and oligoalanine, and studied their conformations by using VCD and ECD spectroscopy. The results indicated that the left-handed helical conformations of oligo(lactic acid)s in these hexamers are indeed rigid and also induce PPII helix formation of adjacent oligoalanine moieties. The chiroptical spectra were analyzed in an empirical manner, because our preliminary DFT (density functional theory) geometry optimization calculations of the oligoalanine moiety of these hexamers resulted in β-strand, not PPII, conformations.

3-2 Results and Discussion

Synthesis and General Properties of Hexamers

Several hexamers were synthesized by combining a Lac trimer and Ala trimer as listed in Table 1. ^{L}Ala trimer was placed before or after ^{L}Lac trimer (**3** and **4**) to study the difference in the influences in the peptide conformation. Using ^{D}Lac and ^{L}Ala, diastereomeric **Ac-^{L}Ala$_3$-^{D}Lac$_3$-OMe** (**5**) and **Ac-^{D}Lac$_3$-^{L}Ala$_3$-OMe** (**6**) were also synthesized to examine the influences of the helicity of Lac trimer on the conformation of ^{L}Ala trimer. **H-^{L}Ala$_6$-OBn** (**2a**) was used as a standard hexaalanine because the other ^{L}Ala hexamers synthesized in this study were not soluble enough for spectral measurements in water (pH 1 to 13), CH_3OH, trifluoroethanol, DMF, $CHCl_3$, and so on. Some oligoalanines have been known difficult to dissolve because of aggregate formations.[13]

Table 1. The structures of the hexamers

	Structure [a]
1 (R^1 = Ac) **1a** (R^1 = Me)	R^1-^{L}Lac$_6$-OMe
2a	H-^{L}Ala$_6$-OBn
3 (R^1 = Ac, R^2 = OMe) **3a** (R^1 = H, R^2 = OH)	R^1-^{L}Ala$_3$-^{L}Lac$_3$-R^2
4	Ac-^{L}Lac$_3$-^{L}Ala$_3$-OMe
5	Ac-^{L}Ala$_3$-^{D}Lac$_3$-OMe
6	Ac-^{D}Lac$_3$-^{L}Ala$_3$-OMe

Ala = -NHCH(CH_3)CO-; Lac = -OCH(CH_3)CO-; Bn = -CH_2Ph

Conformations of the oligoester moiety of hexamers

The VCD spectra of **1**, **3**, and **4** were measured first in $CDCl_3$ and CD_3CN to analyze the conformation of the oligoester moiety through comparison with previously studied

1a in $CDCl_3$.[23] Especially, we were interested to see, if any, differences in the helicity of **3** and **4**, as an ester C=O is capable of acting as a weak hydrogen bond acceptor with an NH group.

As shown in Figure 1a, ^{L}Lac hexamer **1** measured in $CDCl_3$ (gray line) and CD_3CN (black line) exhibited a strong IR and VCD signals in the ester C=O stretching region at around 1750 cm^{-1}. In accordance with our previous observation on **1a**, the negative-positive VCD couplet (from lower to higher frequencies) suggested a left-handed helical structure.[22-25] Meanwhile, heterogeneous hexamers **3** and **4** in CD_3CN presented three characteristic IR absorption bands originating from ester C=O stretching (~1750 cm^{-1}), amide I (~1675 cm^{-1}), and amide II vibrational modes (~1525 cm^{-1}) (black lines in Figure 1b and 1c, Table 2). The $\Delta\varepsilon$ values of the ester carbonyl VCD couplet of **3** and **4** were smaller than those of **1**, as expected from the smaller numbers of ester linkages (seven, four, and three consecutive ester linkages for **1**, **3**, and **4**, respectively). Nonetheless, both **3** and **4** exhibited a negative-positive couplet, which is indicative of the left-handed helical properties of their ^{L}Lac$_3$ moiety. No shift was recognized for the ester C=O IR peak positions between **1** and **3** (1755 cm^{-1}), which should reflect the absence of hydrogen bonds involving ester C=O groups (Table 2). A minor red-shift observed for **4** (1747 cm^{-1}) seemed within a range of red-shifts intrinsic to shorter oligo(lactic acid)s.[23] Possibilities of significant hydrogen bonds involving the ester groups of **4** were also excluded by the similar VCD patterns between **3** and **4** in the amide I and II regions. These observations led us to speculate that the ^{L}Lac$_3$ moieties of **3** and **4** were hardly involved in hydrogen bonding with their ^{L}Ala$_3$ moieties and maintained left-handed helical properties.

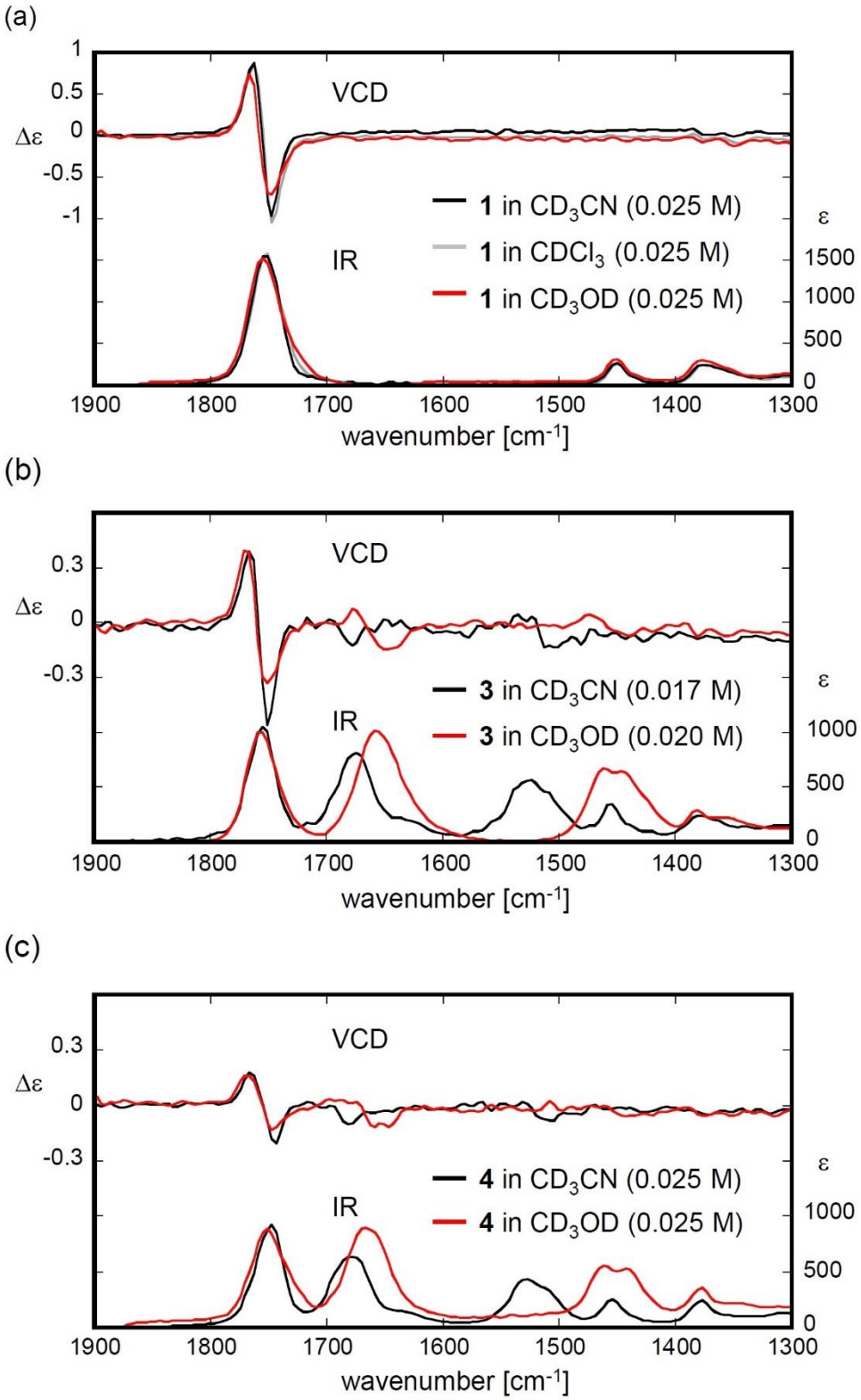

Figure 1. VCD (top) and IR (bottom) spectra of (a) 1, (b) 3, and (c) 4 in CD_3CN (black), CD_3Cl (gray), and CD_3OD (red).

Table 2. Comparison of the peak positions of the exciton couplets of hexamers

	1		3		4		5	6
Solvent	CD_3CN	CD_3OD	CD_3CN	CD_3OD	CD_3CN	CD_3OD	CD_3CN	CD_3CN
ester C=O stretching								
ν [cm^{-1}] at IR_{max}	1755	1759	1755	1759	1747	1751	1755	1747
ν [cm^{-1}] at $\Delta\varepsilon_1$ [a]	1751	1751	1744	1751	1744	1747	1767	1767
ν [cm^{-1}] at $\Delta\varepsilon_2$ [a]	1767	1767	1763	1771	1767	1767	1751	1744
amide I or I'								
ν [cm^{-1}] at IR_{max}	-	-	1674	1659	1678	1667	1674	1682
ν [cm^{-1}] at $\Delta\varepsilon_1$ [a]	-	-	1678	1643	1862	1659 [b]	(1678) [c]	(1682) [c]
ν [cm^{-1}] at $\Delta\varepsilon_2$ [a]	-	-	-	1682	-	1678 [b]		

[a]Wavenumber at the extrema of the first or second Cotton effect ($\Delta\varepsilon_1$ or $\Delta\varepsilon_2$, respectively). [b]Determined by the measurement at 0.017 M. [c]The first Cotton effect appeared at the same or higher frequencies compared to the IR peak maximum.

Conformations of the oligopeptide moiety of hexamers

We then investigated the influence of $^{L}Lac_3$ moiety to the conformation of $^{L}Ala_3$ moiety in more physiologically-relevant, protic solvents. The hexamers listed in Table 1 could not be dissolved in pure water, but most of these were soluble enough for VCD measurement in methanol and ECD measurement in 50% CH_3OH-H_2O. ^{L}Ala hexamer **2a** was studied only by ECD spectroscopy due to its poor solubility. When measured in 50% CH_3OH-H_2O, **2a** exhibited an ECD spectral shape that resembled to β-strand (Figure 2a).[26] The ECD spectral shape of **2** is similar to that of H-$^{L}Ala_6$-OMe,[27] indicating little contribution from the C-terminal benzyl group to its ECD spectral shape.

The conformations of **1**, **3**, and **4** in CD_3OD were then studied by VCD spectroscopy (Figure 1, red line). The VCD signals of their ester carbonyl groups were slightly broadened possibly because of interactions with solvent, but, as expected, maintained

negative-positive patterns. The amide C=O stretching (amide I') of **3** and **4** also presented a negative first Cotton effect and a weak positive second Cotton effect. These results suggested the left-handed helical tendencies of both the triester and tripeptide moieties in **3** and **4**.

The tripeptide conformations were further studied by ECD spectroscopy. As shown in Figure 2b and 2c, **3** and **4** in 50% CH_3OH-H_2O at 25 °C exhibited a positive band at ~217 nm and a negative band at ~193 nm, which are characteristic to PPII helix.[28] Therefore, substitution of amide linkage in ^{L}Ala hexamers to ester linkage increased the conformational propensity of the oligopeptide moiety to form a PPII-like structure. In a similar manner to other reported ^{L}Ala oligomers,[7,8] **3** and **4** underwent helix-strand transition upon increasing temperature with the helix of **3** being slightly more stable than that of **4**, as evidenced by ECD spectroscopy.

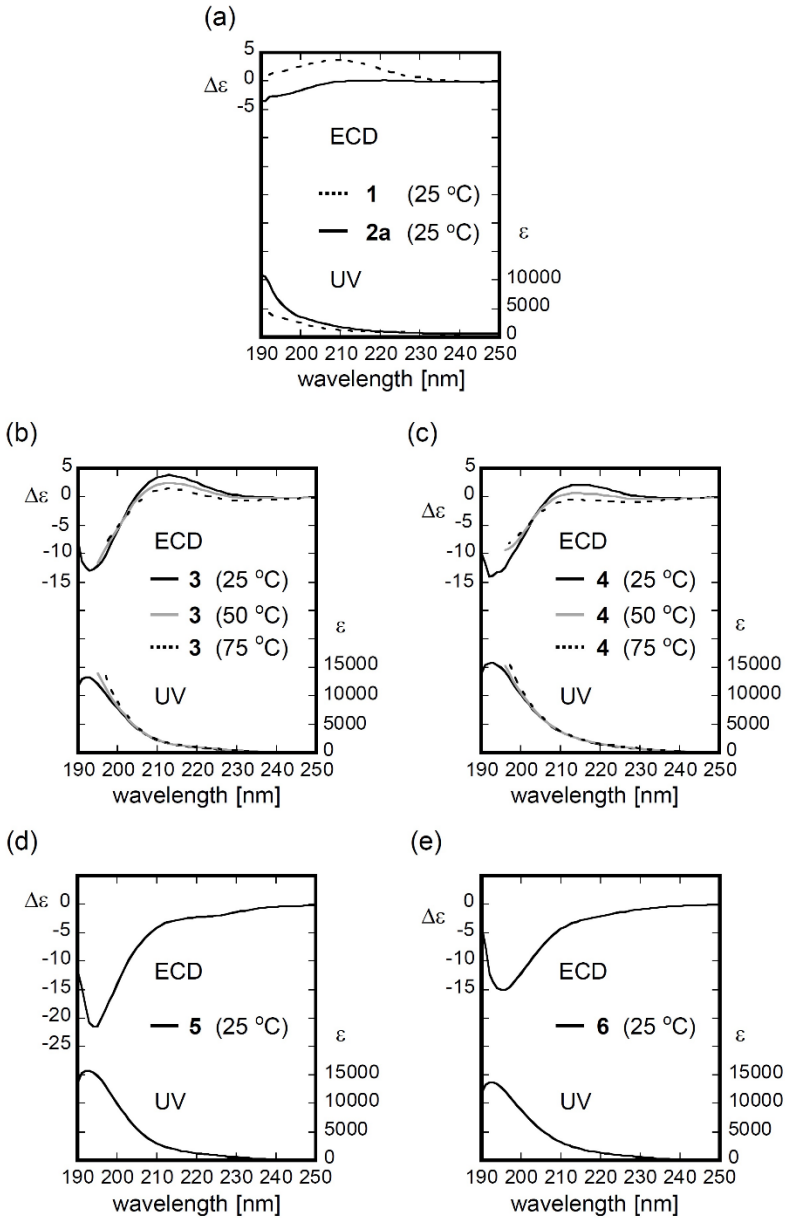

Figure 2. ECD (top) and UV (bottom) spectra of (a) **1** and **2a**, (b) **3**, (c) **4**, (d) **5**, and (e) **6** in 50% CH_3OH-H_2O measured at various temperatures.

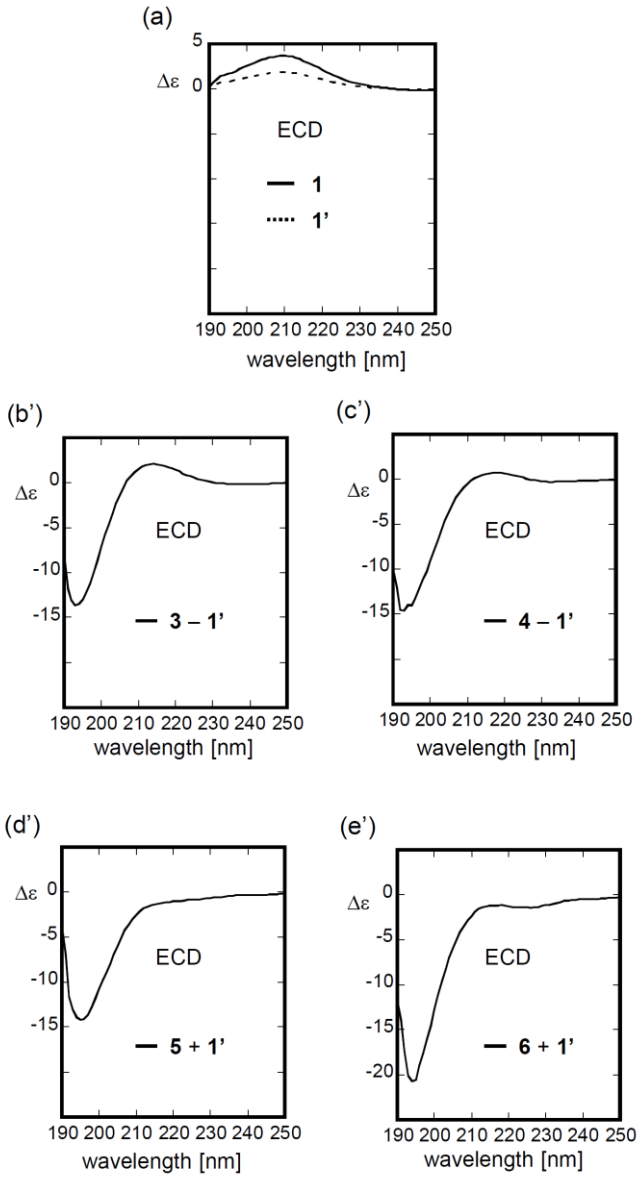

Figure 3. Difference ECD spectra of the ester-containing oligopeptides. (a) In order to eliminate the ECD contribution from the Lac_3 moiety to the spectra of **3**-**6**, the ECD spectrum of the $^{L}Lac_3$ moiety (**1'**) was roughly approximated as that of **1** with half the magnitude. Elimination of the ECD contribution of $^{D}Lac_3$ was carried out by adding **1'** to each spectrum. Simulated ECD spectra of (b) **3**, (c) **4**, (d) **5**, and (e) **6**.

Influence of the helicity of oligoester moiety to oligopeptide moiety

Left-handed helical $^{L}Lac_3$ stabilized a left-handed PPII-like conformation of an adjacent $^{L}Ala_3$. This finding interested us to study which $^{L}Ala_3$ conformation (e.g. left-handed PPII, right-handed α-helix, and β-strand) is induced by inversion of the helicity of the oligoester moiety. To this end, we studied the conformations of hexamers **5** and **6**, of which the right-handed helicity of the $^{D}Lac_3$ moiety was confirmed by VCD measurement (Table 2 and Figure 4). The ECD measurements of **5** and **6** were carried out in 50% CH_3OH-H_2O, resulting in a spectral pattern indicative of a β-strand structure (Figure 2d and 2e). [27] Although right-handed helical $^{D}Lac_3$ could not induce a right-handed helical $^{L}Ala_3$ conformation, this study showed the importance of the combination of the chirality of oligoester and oligopeptide moieties.

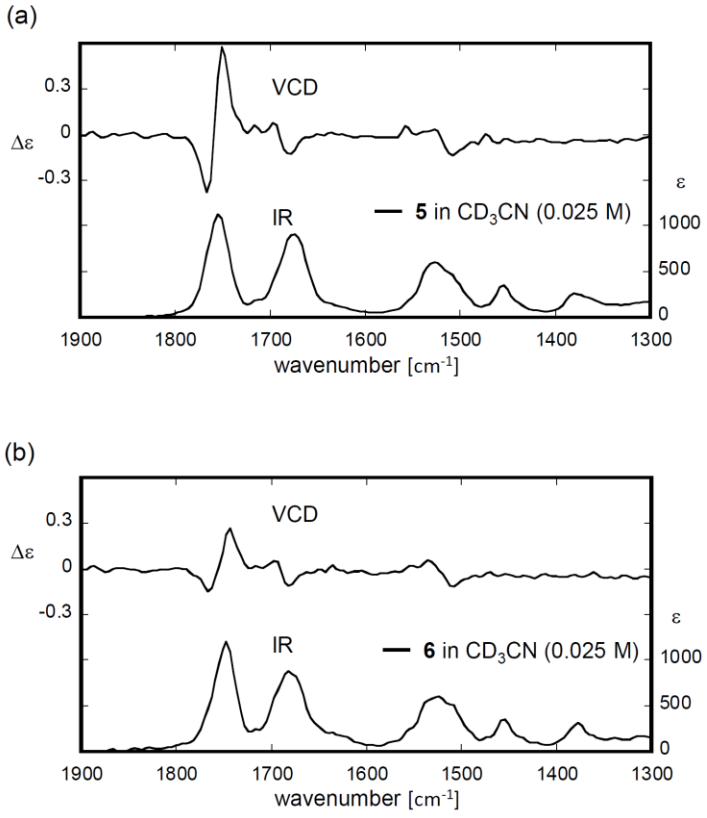

Figure 4. VCD (top) and IR (bottom) spectra of (a) **5** and (b) **6** in CD_3CN.

Application for biological assay

Aiming at future applications of ester-substituted oligopeptides in various biological fields, we first carried out a cell viability assay of H-^{L}Ala$_3$-^{L}Lac$_3$-OH (**3a**) against mouse embryonic fibroblast cells and confirmed that it was indeed low in toxicity (Figure 5). Initially, we also planned to test the antifreeze activity (an activity to inhibit the growth of ice crystal at low temperature) of the hexamers synthesized in this work because of their expected conformational similarity with an AFGP hexapeptide that forms a PPII helix.[14] However, this plan was abandoned due to the insolubility of **3a** in pure water. Despite this observation, **3a** showed much higher solubility than **2a** and H-^{L}Ala$_6$-OH in various solvents such as CH_3OH, 50% CH_3OH-H_2O, and acetonitrile, which exemplified the usefulness of ester substitution for modifications of oligopeptide properties. In order to obtain more insights into the properties of ester-containing peptides, the conformations of the hexamers were further studied.

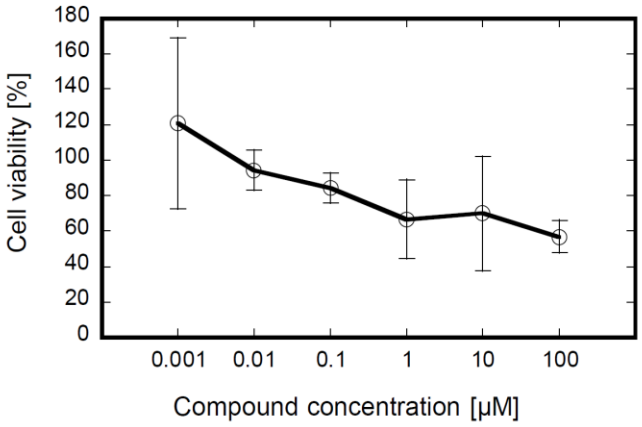

Figure 5. Viability assays of MEF-WT cells exposed to **3'** (H-^{L}Ala$_3$-^{L}Lac$_3$-OH).

3-3 Conclusions

In this work, we incorporated oligo(lactic acid)s, a rigid structural motif we previously found, into ^{L}Ala hexamer sequences, and studied their conformations. These model compounds themselves may be difficult to use for biological systems due to the poor solubility to pure water, albeit low toxicity; however, this study provided useful insights into future applications of ester-substituted oligoesters. First, oligo(L-lactic acid) sequences maintained a left-handed helical structure even when incorporated into oligopeptides. Second, left-handed helical ^{L}Lac$_3$ induced the formation of a left-handed PPII-like helix of adjacent ^{L}Ala$_3$ on both the N- and C-terminal sides. Third, the chirality of oligoester sequences is important for the conformational outcome of neighboring oligopeptides. Last, introduction of ester linkage to oligoalanine increased its solubility to various solvents possibly due to suppression of aggregation.

3-4 Experimantal Section

Cell-Viability Assay (Cell Counting Kit-8 assay): Cells were cultured in Dalbecco's Modified Eagle's Medium (high glucose, D-6429, with 4500 mg/L glucose, L-glutamate, sodium pyruvate, and sodium hydrogen carbonate, obtained from Sigma) with fetal bovine serum (10%; obtained from Gibco), penicillin (50 U/mL), and streptomycin (50 mg/mL; obtained from Sigma). Cells were cultivated at 34 °C under a 5% CO_2 humidified atmosphere.

Mouse embryonic fibroblast cell (1.6×10^4 cells/well) was incubated for 24 h on 96-well plate. Compound **3'** in DMSO was added to the cells with the final concentration of DMSO being 0.1 %. After 24 h, 10 μL of Cell Counting Kit-8 Solution (Dojindo Molecular Technologies, Inc.) was added. After 5 h, Absorbance at 450 nm was measured and cell viability was calculated using the following formula:

$$\text{Viability (\%)}\ \frac{A_s - A_b}{A_c - A_b} \times 100$$

A_s: Absorbance of a sample well; A_c: Absorbance of a negative control well without **3'**; A_b: Absorbance of blank medium well without cells and **3'**. The results of the average of 4 wells for each concentration are shown.

General Procedures.

^{1}H NMR (500 MHz) and ^{13}C NMR (125 MHz) spectra were recorded on a Varian NMR instrument. Chemical shift values are reported in (ppm) values, and coupling constant values (*J*) are in Hertz (Hz). The following abbreviations were used for signal multiplicities: s = singlet; d = doublet; t = triplet; q = quartet; m = multiplet. Electrospray ionization mass spectra were obtained by a JEOL JMS-T100LP spectrometer. Optical rotations were measured on a JASCO P-1020 polarimeter at the sodium D-line using a

1-cm optical cell under ambient temperature, and reported as $[\alpha]_D$ (concentration in grams/100 mL solvent). TLC was performed on 0.2 mm silica gel plates (Merck 60 F254). Column chromatography was carried out on silica gel (Kanto60N, 40-50 μm).

(a) General procedure for ester coupling

To a stirred solution of carboxyl acid and alcohol (or amine) in DMF (1.7 mL/mmol) at rt, 1.5-2.0 equiv of HATU, HOBt, and DIPEA were added. After 3 to 24 h, the mixture was diluted with EtOAc, washed sequentially with 10% citric acid aq, sat $NaHCO_3$ aq, and sat NaCl aq, and then dried over $MgSO_4$. After removal of the solvent under reduced pressure, the crude mixture was purified by column chromatography (hexane/EtOAc solvent system).

(b) General procedure for removal of Benzyl protecting group

A THF solution of Bn-protected compound (6.0 mL/mmol) was added a catalytic amount of 20% $Pd(OH)_2$ and stirred under H_2 atmosphere at rt. After 1.5 to 3 h, the mixture was diluted with EtOAc, filtered through Celite to remove 20% $Pd(OH)_2$. Removal of the solvent from the filtrate under reduced pressure yielded the pure debenzylated product.

(c) General procedure for removal of THP protecting group

To a stirred solution of a THP-protected compound in MeOH (6.0 mL/mmol) at rt, 0.01-0.02 equiv of *p*-TsOH was added. After 2 h, the mixture was diluted with EtOAc, washed sequentially with sat $NaHCO_3$ aq and sat NaCl aq, and then dried over $MgSO_4$. After removal of the solvent under reduced pressure, the residue was subjected to column chromatography (hexane/EtOAc solvent system) to yield the THP-deprotected product.

(d) General procedure for deprotection of Boc protecting group

A Boc-protected compound in HCl in dioxane (4.0 mL/mmol) was stirred at rt. After 30 mins, the solvent was removed under reduced pressure and yielded the Boc-deprotected compound.

(e) General procedure for methyl esterification of carboxyl group

To a stirred solution of carboxyl acid in MeOH (6.0 mL/mmol) at rt, 2.0-3.0 equiv of TMS-diazomethane was then added. After 10 mins, the mixture was evaporated under reduced pressure, and then purified by column chromatography ($CHCl_3$/MeOH solvent systems).

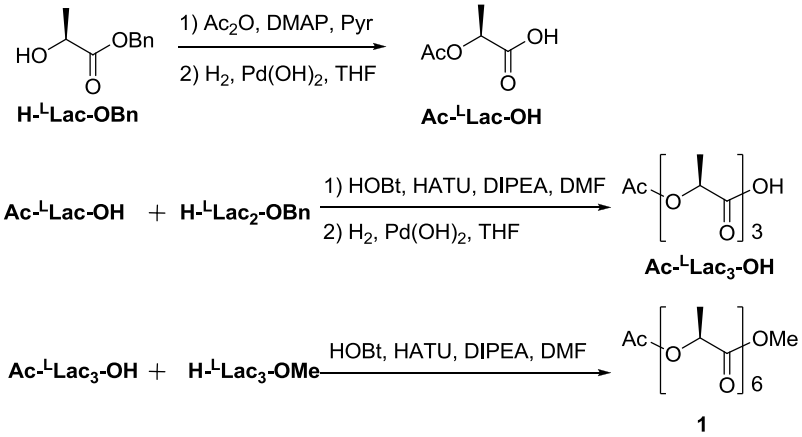

H-^{L}Lac-OBn[23] (424 mg, 2.4 mmol) in pyridine (3.0 mL) was added Ac_2O (450 μL, 2.0 equiv.) and DMAP (29 mg, 0.1 equiv.), and then the mixture was stirred 1 h at rt. The mixture was diluted with EtOAc, washed sequentially with 2N HCl aq, sat $NaHCO_3$ and NaCl aq, and then dried over $MgSO_4$. Removal of the solvent afforded pure Ac-^{L}Lac-OBn (473 mg, 91% yield). The ^{1}H NMR spectrum was identical with that reported in ref 29.

Following the general procedure (b), Ac-^{L}Lac-OBn (463 mg, 2.1 mmol) was converted to Ac-^{L}Lac-OH[29] (274 mg, 99%). Following the general procedure (a), Ac-^{L}Lac-OH (83 mg, 0.63 mmol) and H-^{L}Lac$_2$-OBn[23] (144 mg, 0.57 mmol) were coupled to produce Ac-^{L}Lac$_3$-OBn.[30] Following the general procedure (b), Ac-^{L}Lac$_3$-OBn was converted to Ac-^{L}Lac$_3$-OH[31] (93 mg, 57% in 4 steps). Following the general procedure (a), Ac-^{L}Lac$_3$-OH (21 mg, 0.077 mmol) and H-^{L}Lac$_3$-OMe[23] (19 mg, 0.076 mmol) were coupled to produce **1** (18 mg, 47%). **1**: ^{1}H NMR ($CDCl_3$) δ 5.24-5.09 (m, 6H, CH), 3.75 (s, 3H, OCH_3), 2.13 (s, 3H, CH_3), 1.62-1.57 (m, 12H, CH_3), 1.56 (d, J = 7.1 Hz, 3H, CH_3), 1.52 (d, J = 7.1 Hz, 3H, CH_3). ^{13}C NMR ($CDCl_3$) δ 170.5, 170.4, 170.3, 169.7, 169.6, 169.6, 169.6 (C=O), 69.2, 69.0, 69.0, 68.9, 68.9, 68.3 (CH), 52.4 (OCH_3), 20.6, 16.8, 16.8, 16.7, 16.7, 16.6, 16.6 (CH_3). ESI-MS m/z: $[M + Na]^+$ calcd $C_{21}H_{30}NaO_{14}$ 529.2, found 529.3. $[\alpha]_D$ -81.3 (c 0.1, $CHCl_3$).

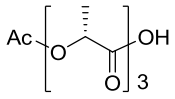

Ac-^{D}Lac-OH was prepared from H-^{D}Lac-OBn in a similar manner to the synthesis of Ac-^{L}Lac-OH (77% yield in 2 steps). THP-^{D}Lac-OH was prepared from H-^{D}Lac-OBn in a similar manner to the synthesis of THP-^{L}Lac-OH (74% yield in 2 steps).[31] Ac-^{D}Lac$_3$-OH was prepared using THP-^{D}Lac-OH, H-^{D}Lac-OBn, and Ac-^{D}Lac-OH in a similar manner to the synthesis of Ac-^{L}Lac$_3$-OH (38% yield in 4 steps). The ^{1}H NMR spectrum was identical with that of Ac-^{L}Lac$_3$-OH. $[\alpha]_D$ +79.9 (c 0.1, $CHCl_3$)

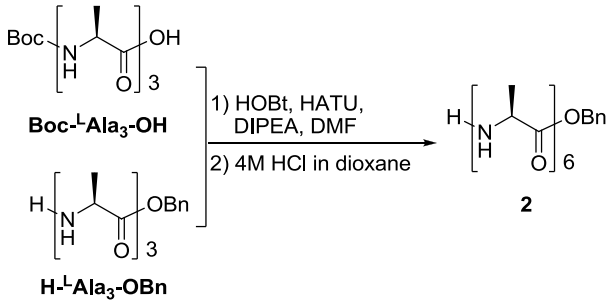

Boc-^{L}Ala$_3$-OH and H-^{L}Ala$_3$-OBn were prepared in a similar procedure reported in ref 32 and 33. Following the general procedure (a), Boc-Ala$_3$-OH and H-^{L}Ala$_3$-OBn were coupled to obtain Boc-^{L}Ala$_6$-OBn. Following the general procedure (d), Boc-^{L}Ala$_6$-OBn was converted to **2**. The NMR spectrum was identical with that reported in ref 34.

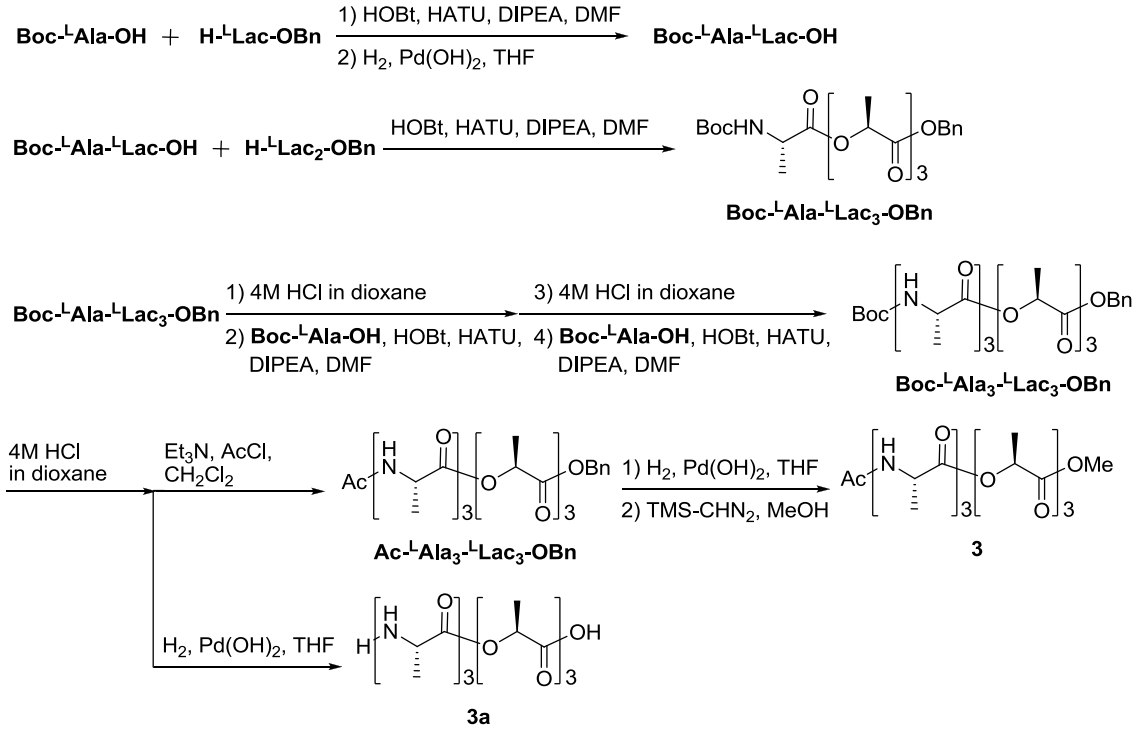

Following the general procedure (a), Boc-^{L}Ala-OH (230 mg, 1.22 mmol) and H-^{L}Lac-OBn (183 mg 1.02 mmol) were coupled to produce Boc-^{L}Ala-^{L}Lac-OBn. The NMR spectrum was identical with that reported in ref 8. Following the general procedure (b), Boc-^{L}Ala-

^{L}Lac-OBn was converted to Boc-^{L}Ala-^{L}Lac-OH. Then, following the general procedure (a), Boc-^{L}Ala-^{L}Lac-OH and H-^{L}Lac$_2$-OBn were coupled to produce Boc-^{L}Ala-^{L}Lac$_3$-OBn (236 mg 57% in 3 steps). **Boc-^{L}Ala-^{L}Lac$_3$-OBn**: ^{1}H NMR ($CDCl_3$) δ 7.39-7.30 (m, 5H, ArH), 5.25-5.12 (m, 5H, CH and PhC$\underline{H}_2$), 5.04-4.96 (br, 1H, NH), 4.43-4.33 (br, 1H, CH), 1.59 (d, J = 7.2 Hz, 3H, CH_3), 1.54-1.51 (m, 6H, CH_3), 1.47-1.43 (m, 12H, CH_3). ^{13}C NMR ($CDCl_3$) δ 169.9, 169.6 (C=O), 135.1, 128.6, 128.5, 128.2 (Ph), 69.3, 68.9, 68.8 (CH), 67.2 (Ph$\underline{C}H_2$), 48.9 (CH), 28.3, 18.4, 16.8, 16.7, 16.6 (CH_3). ESI-MS m/z: $[M + Na]^+$ calcd $C_{21}H_{27}NNaO_9$ 518.2, found 518.3. $[\alpha]_D$ -63.2 (c 0.1, $CHCl_3$).

Boc-^{L}Ala-^{L}Lac$_3$-OBn (205 mg, 0.42 mmol) was converted to Boc-^{L}Ala$_3$-^{L}Lac$_3$-OBn by sequentially following the general procedure (b), (a), (b), and (a) (120 mg, 47% in 4 steps). **Boc-^{L}Ala$_3$-^{L}Lac$_3$-OBn**: ^{1}H NMR ($CDCl_3$) δ 7.40-7.31 (m, 5H, ArH), 6.71-6.62 (m, 2H, NH), 5.23-5.12 (m, 5H, CH and PhC$\underline{H}_2$), 5.02-4.95 (br, 1H, NH), 4.60 (quin, J = 7.2 Hz, 1H, CH), 4.48 (quin, J = 7.1 Hz, 1H, CH), 4.20-4.12 (br, 1H, CH), 1.59 (d, J = 7.2 Hz, 3H, CH_3), 1.55-1.51 (m, 6H, CH_3), 1.48 (d, J = 7.2 Hz, 3H, CH_3), 1.45 (s, 9H, CH_3), 1.39 (d, J = 6.9 Hz, 3H, CH_3), 1.36 (d, J = 7.2 Hz, 3H, CH_3). ^{13}C NMR ($CDCl_3$) δ 172.4, 172.1, 171.5, 171.0, 169.9, 169.8, 169.5 (C=O), 135.1, 128.6, 128.5, 128.2 (Ph), 69.3, 69.0, 69.0 (CH), 67.2 (Ph$\underline{C}H_2$), 50.4, 48.7, 48.0 (CH), 28.3, 18.3, 18.0, 16.7, 16.7, 16.7 (CH_3). ESI-MS m/z: $[M + Na]^+$ calcd $C_{30}H_{43}N_3NaO_{12}$ 660.3, found 660.3. $[\alpha]_D$ -93.2 (c 0.1, $CHCl_3$).

Following the general procedure (d), Boc-^{L}Ala$_3$-^{L}Lac$_3$-OBn (138 mg, 0.22 mmol) was converted to H-^{L}Ala$_3$-^{L}Lac$_3$-OBn. H-^{L}Ala$_3$-^{L}Lac$_3$-OBn in DCM (2.0 mL) was added Et_3N (45 μL, 2.2 equiv.) and AcCl (11 μL, 1.1 equiv.), and stirred 1 h at rt. The mixture was then diluted with $CHCl_3$, washed sequentially with 2N HCl aq, sat $NaHCO_3$ aq and NaCl aq, and then dried over $MgSO_4$. After removal of the solvent, the residue was purified by column chromatography ($CHCl_3$:MeOH = 15:1), which afforded Ac-^{L}Ala$_3$-^{L}Lac$_3$-OBn. (49

mg, 65 in 2 steps) **Ac-^{L}Ala$_3$-^{L}Lac$_3$-OBn**: ^{1}H NMR ($CDCl_3$) δ 7.40-7.25 (m, 7H, ArH and NH), 6.80 (d, *J* = 7.8 Hz, 1H, NH), 5.21-5.10 (m, 5H, CH and PhC$\underline{H}_2$), 4.70-4.55 (m, 3H, CH), 2.01 (s, 3H, CH_3), 1.59 (d, *J* = 7.2 Hz, 3H, CH_3), 1.54-1.51 (m, 6H, CH_3), 1.49 (d, *J* = 7.2 Hz, 3H, CH_3), 1.39 (d, *J* = 6.9 Hz, 3H, CH_3), 1.36 (d, *J* = 6.9 Hz, 3H, CH_3). ^{13}C NMR ($CDCl_3$) δ 172.3, 171.2, 171.9, 170.0, 169.9, 169.8, 169.5 (C=O), 135.0, 128.6, 128.5, 128.2 (Ph), 69.3, 69.0, 68.9 (CH), 67.2 (Ph$\underline{C}H_2$), 48.7, 47.9 (CH), 23.1, 19.2, 18.9, 17.8, 16.7, 16.6 (CH_3). ESI-MS m/z: $[M + Na]^+$ calcd $C_{27}H_{37}N_3NaO_{11}$ 602.2, found 602.3. $[\alpha]_D$ -100.4 (c 0.1, $CHCl_3$).

Following the general procedure (b) and (e), Ac-^{L}Ala$_3$-^{L}Lac$_3$-OBn was converted to Ac-^{L}Ala$_3$-^{L}Lac$_3$-OH and then to **3** (23 mg, 70% in 2 steps). **3**: ^{1}H NMR ($CDCl_3$) δ 7.12-7.07 (m, 2H, NH), 6.62 (d, *J* = 7.4 Hz, 1H, NH), 5.20-5.13 (m, 3H, CH), 4.65-4.57 (m, 3H, CH), 3.75 (s, 3H, OCH_3), 2.02 (s, 3H, CH_3), 1.62-1.58 (m, 6H, CH_3), 1.52 (d, *J* = 7.1 Hz, 3H, CH_3), 1.50 (d, *J* = 7.1 Hz, 3H, CH_3), 1.40 (d, *J* = 7.1 Hz, 3H, CH_3), 1.37 (d, *J* = 6.8 Hz, 3H, CH_3). ^{13}C NMR ($CDCl_3$) δ 172.2, 172.2, 171.7, 170.5, 170.0, 169.8, 169.6 (C=O), 69.2, 69.0, 69.0 (CH), 52.5 (OCH_3), 48.9, 48.8, 47.9 (CH), 23.1, 19.0, 18.7, 17.9, 16.8, 16.7, 16.6 (CH_3). ESI-MS m/z: $[M + Na]^+$ calcd $C_{21}H_{33}N_3NaO_{11}$ 526.2, found 526.2. $[\alpha]_D$ -64.4 (c 0.1, $CHCl_3$).

Following the general procedure (b), H-^{L}Ala$_3$-^{L}Lac$_3$-OBn was converted to **3a** (20 mg, 65%). ESI-MS m/z: $[M + H]^+$ calcd $C_{18}H_{30}N_3O_{10}$ 448.2, found 448.2.).

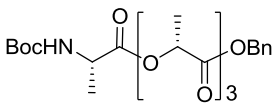

Boc-^{L}Ala-^{D}Lac$_3$-OBn was prepared using Boc-^{L}Ala-OH, H-^{D}Lac-OBn, and H-^{D}Lac$_2$-OBn in a similar manner to the synthesis of Boc-^{L}Ala-^{L}Lac$_3$-OBn (35% yield in 3 steps). **Boc-^{L}Ala-^{D}Lac$_3$-OBn**: ^{1}H NMR ($CDCl_3$) δ 7.40-7.32 (m, 5H, ArH), 5.25-5.12 (m, 5H, CH and

PhC<u>H</u>$_2$), 5.08-5.02 (br, 1H, NH), 4.44-4.36 (br, 1H, CH), 1.58 (d, J = 6.9 Hz, 3H, CH_3), 1.55-1.51 (m, 6H, CH_3), 1.47-1.41 (m, 12H, CH_3). ^{13}C NMR ($CDCl_3$) δ 172.5, 171.1, 171.0, 169.9, 169.6 (C=O), 135.0, 128.6, 128.5, 128.2 (Ph), 69.2, 69.0, 68.9 (CH), 67.2 (Ph<u>C</u>H$_2$), 49.4 (CH), 28.3, 18.5, 16.8, 16.7, 16.6 (CH_3). ESI-MS m/z: $[M + Na]^+$ calcd $C_{21}H_{27}NNaO_9$ 518.2, found 518.3. $[\alpha]_D$ +46.1 (c 0.1, $CHCl_3$).

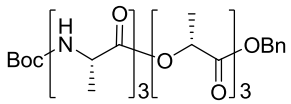

Boc-^{L}Ala$_3$-^{D}Lac$_3$-OBn was prepared from Boc-^{L}Ala-^{D}Lac$_3$-OBn in a similar manner to the synthesis of Boc-^{L}Ala$_3$-^{L}Lac$_3$-OBn (57% in 4 steps). **Boc-^{L}Ala$_3$-^{D}Lac$_3$-OBn**: ^{1}H NMR ($CDCl_3$) δ 7.40-7.31 (m, 5H, ArH), 6.73-6.67 (m, 2H, NH), 5.23-5.12 (m, 5H, CH and PhC<u>H</u>$_2$), 5.03-4.97 (br, 1H, NH), 4.63 (quin, J = 7.2 Hz, 1H, CH), 4.47 (quin, J = 7.1 Hz, 1H, CH), 4.20-4.12 (br, 1H, CH), 1.58 (d, J = 6.9 Hz, 3H, CH_3), 1.55-1.52 (m, 6H, CH_3), 1.47-1.43 (m, 12H, CH_3), 1.38 (d, J = 7.2 Hz, 3H, CH_3), 1.36 (d, J = 6.9 Hz, 3H, CH_3). ^{13}C NMR ($CDCl_3$) δ 172.4, 171.7, 171.4, 169.9, 169.7, 169.7 (C=O), 135.0, 128.6, 128.6, 128.3 (Ph), 69.3, 69.1, 69.0 (CH), 67.3 (Ph<u>C</u>H$_2$), 50.3, 48.7, 48.2 (CH), 28.3, 18.2, 17.9, 16.8, 16.7, 16.6, 16.6 (CH_3). ESI-MS m/z: $[M + Na]^+$ calcd $C_{30}H_{43}N_3NaO_{12}$ 660.3, found 660.3. $[\alpha]_D$ -11.1 (c 0.1, $CHCl_3$).

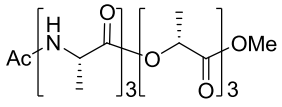

5 was prepared from Boc-^{L}Ala$_3$-^{D}Lac$_3$-OBn in a similar manner to the synthesis of **3** (42% yield in 4 steps). **Ac-^{L}Ala$_3$-^{D}Lac$_3$-OBn**: ^{1}H NMR ($CDCl_3$) δ 7.40-7.30 (m, 5H, ArH), 7.28-7.19 (br, 2H, NH), 6.82-6.74 (br, 1H, NH), 5.23-5.17 (m, 5H, CH and PhC<u>H</u>$_2$), 4.69-

4.58 (m, 3H, CH), 2.01 (s, 3H, CH_3), 1.57 (d, J = 6.9 Hz, 3H, CH_3), 1.54-1.50 (m, 3H, CH_3), 1.45 (d, J = 7.2 Hz, 3H, CH_3), 1.39 (d, J = 6.9 Hz, 3H, CH_3), 1.36 (d, J = 6.9 Hz, 3H, CH_3). ^{13}C NMR ($CDCl_3$) δ 172.2, 171.8, 171.7, 170.0, 169.9, 169.6, 169.6 (C=O), 135.0, 128.6, 128.5, 128.2 (Ph), 69.3, 69.0, 69.0 (CH), 67.2 (Ph<u>C</u>H_2), 48.8, 48.7, 48.1 (CH), 23.1, 19.2, 18.9, 17.7, 16.7, 16.7, 16.6 (CH_3). ESI-MS m/z: $[M + Na]^+$ calcd $C_{27}H_{37}N_3NaO_{11}$ 602.2, found 602.3. $[\alpha]_D$ +10.2 (c 0.1, $CHCl_3$).

5: ^{1}H NMR ($CDCl_3$) δ 7.27-7.21 (m, 2H, NH), 6.76 (d, J = 7.4 Hz, 1H, NH), 5.21-5.12 (m, 3H, CH), 4.68-4.59 (m, 3H, CH), 3.75 (s, 3H, OCH_3), 2.02 (s, 3H, CH_3), 1.60 (d, J = 7.1 Hz, 3H, CH_3), 1.58 (d, J = 7.1 Hz, 3H, CH_3), 1.52 (d, J = 7.1 Hz, 3H, CH_3), 1.45 (d, J = 7.1 Hz, 3H, CH_3), 1.39 (d, J = 6.8 Hz, 3H, CH_3), 1.36 (d, J = 6.8 Hz, 3H, CH_3). ^{13}C NMR ($CDCl_3$) δ 172.2, 171.8, 171.7, 170.5, 170.1, 169.6, 169.6 (C=O), 69.2, 69.0, 69.0 (CH), 52.5 (OCH_3), 48.8, 48.7, 48.1 (CH), 23.1, 19.2, 18.9, 17.7, 16.8, 16.7, 16.6 (CH_3). ESI-MS m/z: $[M + Na]^+$ calcd $C_{21}H_{33}N_3NaO_{11}$ 526.2, found 526.2. $[\alpha]_D$ +1.4 (c 0.1, $CHCl_3$).

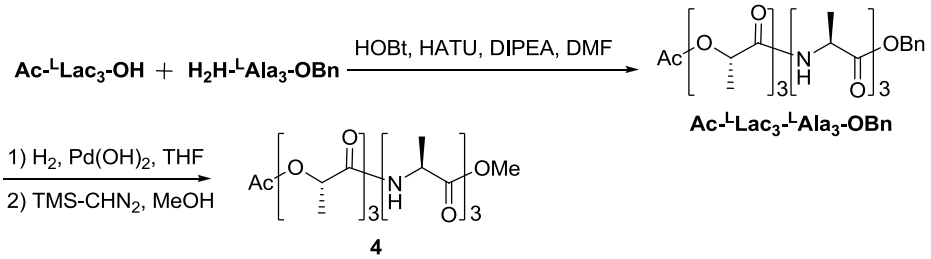

4: Following the general procedure (a), Ac-^{L}Lac$_3$-OH (28 mg, 0.10 mmol) and H-^{L}Ala$_3$-OBn (35 mg 0.10 mmol) were coupled to produce Ac-^{L}Lac$_3$-^{L}Ala$_3$-OBn (28 mg, 48%). **Ac-^{L}Lac$_3$-^{L}Ala$_3$-OBn**: ^{1}H NMR ($CDCl_3$) δ 7.39-7.30 (m, 5H, ArH), 6.84 (d, J = 7.5 Hz, 1H, NH), 6.80 (d, J = 6.6 Hz, 1H, NH), 6.54 (d, J = 7.8 Hz, 1H, NH), 5.21-5.02 (m, 5H, CH and Ph<u>C</u>H_2), 4.58 (quin, J = 7.3 Hz, 1H, CH), 4.48 (quin, J = 7.3 Hz, 1H, CH), 4.39 (quin, J = 7.0 Hz, 1H, CH), 2.15 (s, 3H, CH_3), 1.60 (d, J = 7.2 Hz, 3H, CH_3), 1.56 (d, J = 7.2 Hz, 3H,

CH_3), 1.51 (d, J = 6.9 Hz, 3H, CH_3), 1.46-1.42 (m, 6H, CH_3), 1.38 (d, J = 6.9 Hz, 3H, CH_3). ^{13}C NMR ($CDCl_3$) δ 172.4, 171.8, 171.5, 170.7, 170.4, 169.8, 169.7 (C=O), 135.5, 128.5, 128.2, 128.1 (Ph), 72.4, 70.3, 68.9 (CH), 67.0 (Ph<u>C</u>H_2), 49.5, 48.8, 48.2 (CH), 20.5, 17.9, 17.5, 17.3, 17.2, 16.7, 16.6 (CH_3). ESI-MS m/z: $[M + Na]^+$ calcd $C_{27}H_{37}N_3NaO_{11}$ 602.2, found 602.3. $[\alpha]_D$ -60.7 (c 0.1, $CHCl_3$).

Following the general procedure (b) and (c), Ac-^{L}Lac$_3$-^{L}Ala$_3$-OBn was converted to Ac-^{L}Lac$_3$-^{L}Ala$_3$-OH and then to **4** (9.0 mg, 33% in 3 steps). **4**: ^1H NMR ($CDCl_3$) δ 6.80 (m, 2H, NH), 6.50 (d, J = 7.2 Hz, 1H, NH), 5.12-5.01 (m, 3H, CH), 4.54 (quin, J = 7.4 Hz, 1H, CH), 4.48 (quin, J = 7.3 Hz, 1H, CH), 4.39 (quin, J = 6.7 Hz, 1H, CH), 3.74 (s, 3H, OCH_3), 2.15 (s, 3H, CH_3), 1.61 (d, J = 7.2 Hz, 3H, CH_3), 1.57 (d, J = 6.9 Hz, 3H, CH_3), 1.52 (d, J = 6.9 Hz, 3H, CH_3), 1.45 (d, J = 7.4 Hz, 3H, CH_3), 1.43 (d, J = 7.2 Hz, 3H, CH_3), 1.40 (d, J = 7.2 Hz, 3H, CH_3). ^{13}C NMR ($CDCl_3$) δ 173.1, 171.9, 171.7, 171.6, 171.4, 170.7, 170.5 (C=O), 72.5, 70.4, 68.9 (CH), 52.4 (OCH_3), 49.6, 48.8, 48.1 (CH), 20.5, 17.9, 17.5, 17.2, 17.1, 16.7, 16.6 (CH_3). ESI-MS m/z: $[M + Na]^+$ calcd $C_{21}H_{33}N_3NaO_{11}$ 526.2, found 526.2. $[\alpha]_D$ -55.9 (c 0.1, $CHCl_3$).

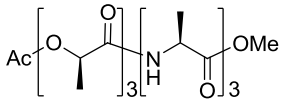

6 was prepared from Ac-^{D}Lac$_3$-OH and H_2N-^{L}Ala$_3$-OBn in a similar manner to the synthesis of **4** (33% yield in 3 steps). **Ac-^{D}Lac$_3$-^{L}Ala$_3$-OBn**: ^1H NMR ($CDCl_3$) δ 7.40-7.30 (m, 5H, ArH), 6.88 (d, J = 7.8 Hz, 1H, NH), 6.82-6.75 (m, 2H, NH), 5.27-5.13 (m, 4H, CH and Ph<u>C</u>H_2), 5.04 (q, J = 7.0 Hz, 1H, CH), 4.56 (quin, J = 7.3 Hz, 1H, CH), 4.48 (quin, J = 7.3 Hz, 1H, CH), 4.37 (quin, J = 7.0 Hz, 1H, CH), 2.14 (s, 3H, CH_3), 1.59 (d, J = 7.2 Hz, 3H, CH_3), 1.57 (d, J = 7.2 Hz, 3H, CH_3), 1.49 (d, J = 6.9 Hz, 3H, CH_3), 1.44-1.41 (m, 6H,

CH_3), 1.35 (d, J = 6.9 Hz, 3H, CH_3). ^{13}C NMR ($CDCl_3$) δ 172.3, 171.7, 171.5, 171.3, 170.9, 170.2, 169.0 (C=O), 135.3, 128.6, 128.4, 128.1 (Ph), 71.3, 69.2, 69.0 (CH), 67.1 (Ph$\underline{C}H_2$), 49.5, 48.7, 48.2 (CH), 20.6, 18.0, 17.7, 17.5, 17.3, 16.7, 16.7 (CH_3). ESI-MS m/z: $[M + Na]^+$ calcd $C_{27}H_{37}N_3NaO_{11}$ 602.2, found 602.3. $[\alpha]_D$ +5.2 (c 0.1, $CHCl_3$).

6: ^1H NMR ($CDCl_3$) δ 6.87 (d, J = 7.4 Hz, 1H, NH), 6.80-6.74 (m, 2H, NH), 5.24 (q, J = 6.9 Hz, 1H, CH), 5.16 (q, J = 7.0 Hz, 1H, CH), 5.04 (q, J = 7.1 Hz, 1H, CH), 4.55-4.44 (m, 2H, CH), 4.38 (quin, J = 7.0 Hz, 1H, CH), 3.75 (s, 3H, OCH_3), 2.15 (s, 3H, CH_3), 1.60 (d, J = 7.1 Hz, 3H, CH_3), 1.57 (d, J = 7.1 Hz, 3H, CH_3), 1.49 (d, J = 7.1 Hz, 3H, CH_3), 1.44 (d, J = 7.4 Hz, 3H, CH_3), 1.42 (d, J = 7.1 Hz, 3H, CH_3), 1.37 (d, J = 7.1 Hz, 3H, CH_3). ^{13}C NMR ($CDCl_3$) δ 173.0, 171.8, 171.5, 171.4, 170.9, 170.2, 169.0 (C=O), 71.3, 69.6, 69.1 (CH), 52.5 (OCH_3), 49.6, 48.7, 48.2 (CH), 20.6, 18.0, 17.6, 17.5, 17.3, 16.7, 16.7 (CH_3). ESI-MS m/z: $[M + Na]^+$ calcd $C_{21}H_{33}N_3NaO_{11}$ 526.2, found 526.2. $[\alpha]_D$ +3.1 (c 0.1, $CHCl_3$).

3-5 References

1. Adzhubei, A. A.; Sternberg, Michael J. E.; Makarov, A. A. *J. Mol. Biol.* **2013**, *425*, 2100-2132.

2. Bochicchio, B.; Tamburro, A. M. *Chirality* **2002**, *14*, 782-792.

3. Yang, L.; Schepartz, A. *Biochemistry* **2005**, *44*, 7469-7478.

4. Kroll, C.; Mansi, R.; Braun, F.; Dobitz, S.; Maecke, H. R.; Wennemers, H. *J. Am. Chem. Soc.* **2013**, *135*, 16793-16796.

5. Ruzza, P.; Siligardi, G.; Donella-Deana, A.; Calderan, A.; Hussain, R.; Rubini, C,; Cesaro, L.; Osler, A.; Guiotto, A.; Pinna, L. A.; Borin, G. *J. Pept. Sci.* **2006**, *12*, 462-471.

6. Pentelute, B. L.; Gates, Zachary, P.; Tereshko, V.; Dashnau, J. L.; Vanderkooi, J. M.; Kossiakoff, A. A.; Kent, S. B. H. *J. Am. Chem. Soc.* **2008**, *130*, 9695-9701.

7. Schweitzer-Stenner, R.; Eker, F.; Griebenow, K.; Cao, X.; Nafie, L. A. *J. Am. Chem. Soc.* **2004**, 126, 2768-2776.

8. Oh, K.-I.; Lee, K.-K.; Park, E.-K.; Yoo, D.-G.; Hwang, G.-S.; Cho, M. *Chirality* **2010**, *22*, E186-E202.

9. McColl, I. H.; Blanch, E. W.; Hecht, L.; Kallenbach, N. R.; Barron, L. D. *J. Am. Chem. Soc.* **2004**, 126, 5076-5077.

10. Yamamoto, S.; Furukawa, T.; Bour, P.; Ozaki, Y. *J. Phys. Chem. A* **2014**, *118*, 3655-3662.

11. Narayanan, U.; Keiderling, T. A.; Bonora, G. M.; Toniolo, C. *Biopolymers* **1985**, *24*, 1257-1263.

12. Kametani, S.; Tasei, Y.; Nishimura, A.; Asakura, T. *Phys. Chem. Chem. Phys.* **2017**, *19*, 20829-20838.

13. Baker, P. J.; Numata, K. *Biomacromolecules* **2012,** *1*, 947-951.

14. Tachibana, Y.; Fletcher, G. L.; Fujitani, N.; Tsuda, S.; Monde, K.; Nishimura, S.-I. *Angew. Chem. Int. Ed.* **2004**, *41*, 856-862.

15. Taniguchi, T.; Monde. K. *Chem.-Asian J.* **2007**, *2*, 1258-1266.

16. Nelli, Y. R.; Fischer, L.; Collie, G. W.; Kauffmann, B.; Guichard, G. *Biopolymers* **2013**, *100*, 687-697.

17. Diedrich, D.; Moita, A. J. R.; Ruether, A.; Frieg, B.; Reiss, G. J.; Hoeppner, A.; Kurz, T.; Gohlke, H.; Luedeke, S.; Kassack, M. U.; Hansen, F.K. *Chem. Eur. J.* **2016**, *22*, 17600-17611.

18. Deechongkit, S.; Nguyen, H.; Powers, E. T.; Dawson, P. E.; Gruebele, M.; Kelly, J. W. *Nature* **2004**, *430*, 101-105.

19. Kobayashi, T.; Yanagisawa, T.; Sakamoto, K.; Yokoyama, S. *J. Mol. Biol.* **2009**, *385*, 1352-1360.

20. Li, Y. M.; Yang, M. Y.; Huang, Y. C.; Li, Y. T.; Chen, P. R.; Liu, L. *ACS Chem. Biol.* **2012**, *7*, 1015-1022.

21. Lee, J.; Jang, G.; Kang, P.; Choi, M. G.; Choi, S. H. *Org. Biomol. Chem.* **2016**, *14*, 8438-8442.

22. Ho, R. M.; Li, M. C.; Lin, S. C.; Wang, H. F.; Lee, Y. D.; Hasegawa, H.; Thomas, E. L. *J. Am. Chem. Soc.* **2012**, *134*, 10974-10986.

23. Hongen, T.; Taniguchi, T.; Nomura, S.; Kadokawa, J.; Monde, K. *Macromolecules* **2014**, *47*, 5313-5319.

24. Taniguchi, T.; Monde, K. *J. Am. Chem. Soc.* **2012**, *134*, 3695-3698.

25. Taniguchi, T.; Hongen, T.; Monde, K. *Polymer J.* **2016**, *48*, 925-931.

26. Shi, Z.; Olson, C. A.; Rose, G. D.; Baldwin, R. L.; Kallenbach, N. R. *Proc. Natl. Acad. Sci. U.S.A.* **2002**, *99*, 9190-9195.

27. Loremi, G. P.; Rizzo, V.; Thoresen, F.; Tomasic, L. *Macromolecules* **1979**, *12*, 870-874.

28. The positive ECD band of **3** and **4** observed at around 217 nm was not due to the ECD signals originating from $^{L}Lac_3$ moiety. See Figure S3.

29. Rioz-Martinez, A.; Cuetos, A.; Rodriguez, C.; de Gonzalo, G.; Lavandera, I.; Fraaije, M. W.; Gotor, V. *Angew. Chem. Int. Ed.* **2011,** *50*, 8387-8390.

30. Zhu, H.; Xu, X.; Cui, W.; Zhang, Y.; Mo, H.; Shen, Y. M. *J. Polym. Sci. A Polym. Chem.* **2011**, *49*, 1745-1752.

31. Cleland, J. L.; Yang, M.; Bauman, J. G.; Hoang, N. *U.S. Pat. Appl. Publ.* **2017**, US 20170080092 A1 20170323.

32. Chandra, K.; Dutta, D.; Das, A. K.; Basak, A. *Bioorg. Med. Chem.* **2010**, *18*, 8365-8373.

33. Sugiyama, Y.; Shirai, R.; Hirose, M.; Watanabe, T.; Yoshida, A.;, Endo, N.; Hayashi, T.; Shioiri, T.; Matsugi, M. *Synthesis* **2017**, *49*, 2187-2204.

34. Graf, J.; Nguyen, P. H.; Stock, G.; Schwalbe, H. *J. Am. Chem. Soc.* **2007**, *129*, 1179-1189.

35. Gilon, C.; Klausner, Y.; Hassner, A. *Tetrahedron Lett.* **1979**, *40*, 3811-3814.

Chapter 4

Concluding Remark

I discussed the potential of VCD spectroscopy for analyzing the configuration and solution-state conformation of bio(macro) molecules and their analogs. Special emphasis was given to the VCD exciton chirality method, which can be employed to elucidate stereostructures that are difficult to study by other methods.

In Chapter 2, VCD spectroscopy has extensively been applied to poly lactic acid, aming at creating novel structural analysis method focusing on their chiral properties. The information obtained here should be beneficial for future applications of oligo(L-lactic acid)s as a rigid structural unit for genetically engineered proteins. In addition, through the work on PLLA and its oligomers, we have demonstrated that a convenient and precise analysis of the conformation of polyester can be achieved by using VCD spectroscopy. The application to other polyesters will be reported in due course. Such structural studies should accelerate further industrial and scientific utility of polyesters.

In chapter 3, I revealed rigid conformation of oligo lactide leads oligoalanine's conformation to PPII helical structure. These insights should be useful in developing peptide analogues containing ester linkage with various amino acids and α-hydroxy acids that function better than normal oligopeptides.

The studies in this thesis suggested that VCD and CD spectroscopy be informative and convenient analytical tools for helical structure. This technique will play an important role in this rapidly progressing polmerscience and peptidomimetics field.

Appendix (Publications)

Original Papers (Related to this thesis)

1. Hongen, T.; Taniguchi, T.; Nomura, S.; Kadokawa, J.; Monde, K.

In Depth Study on Solution-State Structure of Poly(lactic acid) by Vibrational Circular Dichroism

Mcromolecules **2014**, *47*, 5313-5319.

2. Hongen, T.; Taniguchi, T.; Monde, K.

Modifying Oligoalanine Conformation by Replacement of Amide to Ester Linkage

Chirality **2017**, *Accepted*.

Original Review (Related to this thesis)

3. Taniguchi, T.; Hongen, T.; Monde, K.

Studying the stereostructures of biomolecules and their analogs by vibrational circular dichroism

Polymer Journal **2016**, *48*, 925–931.